TITLE:

水素結合による集合体の強相関構造形成の理論構築

AUTHOR(S):

田中, 文彦

CITATION:

田中, 文彦. 水素結合による集合体の強相関構造形成の理論構築. 2004

ISSUE DATE:

2004-03

URL:

http://hdl.handle.net/2433/50613

RIGHT:

p.94-450は、学術雑誌等掲載論文。出版社の著作権許諾が得られていないため、電子化はしていない。

京都大学学術情報リポジトリ
KURENAI 紅
Kyoto University Research Information Repository

「水素結合による集合体の強相関構造形成の理論構築」

Theoretical Study of Strongly-Correlated Structure Formation
in Hydrogen-Bonded Self-Assemblies of Polymers

（課題番号　13031048）

平成１３－１５年度
文部科学省科学研究費補助金（特定領域研究 (2)）

研究成果報告書

平成１６年３月

研究代表者
田　中　文　彦
（京都大学大学院工学研究科高分子化学専攻）
Fumihiko Tanaka
Department of Polymer Chemistry
Graduate School of Engineering
Kyoto University

「水素結合による集合体の強相関構造形成の理論構築」

Theoretical Study of Strongly-Correlated Structure Formation
in Hydrogen-Bonded Self-Assemblies of Polymers

（課題番号　13031048）

平成１３－１５年度
文部科学省科学研究費補助金（特定領域研究 (2)）

研究成果報告書

平成１６年３月

研究代表者
田　中　文　彦
（京都大学大学院工学研究科高分子化学専攻）
Fumihiko Tanaka
Department of Polymer Chemistry
Graduate School of Engineering
Kyoto University

はしがき

この報告書は平成１３年から１５年にわたり交付された文部科学省科学研究費補助金（特定領域研究(2)）により行った研究

「水素結合による集合体の強相関構造形成の理論構築」
（課題番号 13031048）
Theoretical Study of Strongly-Correlated Structure Formation
in Hydrogen-Bonded Self-Assemblies of Polymers

の成果をまとめたものである．研究発表，研究成果の項には補助金交付期間中の２年間に得られた成果をまとめてあるが，巻末の資料には研究課題の着想のもとになった理論的考察に関する一連の論文と，それらを包括するレビュー論文を収録してある．強い相互作用のある高分子系を取り扱う一般的な理論になりつつある「高分子会合溶液理論」をより多くの専門家に周知して頂きたい願いをこめ，また，自分自身でも今後の研究の出発点として使用したかったためである．

高分子の会合現象は疎水性相互作用，水素結合，静電相互作用，およびそれらの協同的効果によってもたらされ，マクロ・ミクロ相分離，ゲル化，ヘリックス・コイル転移，ミセル形成，液晶化等，溶液系で観測される特徴的な相転移現象のほとんどすべてに関与している．我々は 1980 年代後半にアタクチックポリスチレンのゲル化相図の実験報告に啓発され会合溶液の理論的考察を始めたが，1990 年代に入り水溶性会合高分子の形成するミセルや弱いゲル（組み替えネットワーク）の研究のために会合溶液理論を多重架橋体に展開した．さらに 2000 年代に入り本課題を推進するに当たり，これまでの理論を水素結合による高分子のゲル化現象に適用できるように理論を強化した．本課題では特に水素結合の方向性と連鎖性に注目し，水素結合超分子の液晶，水素結合らせん形成によるバイオポリマーのゲル化，キラル分子による水素結合誘起らせん高分子の研究を行った．これらの研究は特定領域研究の期間が終結した現在も継続中である．さらに将来的には第３の，そして天然高分子では最も重要な相互作用である電磁気力による高分子電解質・対イオン系のゲル化現象に向けて展開していく予定である．本報告書が高分子系の関連テーマ研究者の研究推進のための一助となれば幸いである．

平成１６年３月
田中文彦

＜研究組織＞

研究代表者：	田中文彦	（京都大学大学院工学研究科・教授）
研究分担者：	古賀　毅	（京都大学大学院工学研究科・助手）
	庄司雅彦	（京都大学大学院工学研究科・助手）

（庄司は平成１３，１４年度のみ）

＜交付研究経費＞

平成１３年度	４，５００　千円
平成１４年度	５，５００　千円
平成１５年度	５，６００　千円
計	１５，６００　千円

＜目次＞

— 研究概要 —

水素結合による集合体の強相関構造形成の理論構築

田中文彦
京都大学大学院工学研究科・高分子化学専攻
〒615-8510　京都市西京区桂
TEL・FAX: 075-383-2705, e-mail: ftanaka@phys.polym.kyoto-u.ac.jp

概要　水素結合には可逆性，飽和性，特異性，方向性，連鎖性などの特徴があり種々の興味深い空間構造を形成する重要な相互作用である．本課題では，これらの特徴の中で方向性と連鎖性に注目し，高分子系を中心にして水素結合超分子液晶，ヘリックス形成とその凝集による熱可逆ゲル，ジッパー型架橋領域を有する熱可逆ゲル，水素結合誘起らせん高分子，その伸長によるラセミ混合溶液の光学分割，等について統計力学的手法で研究した．

1　はじめに

近年我々は高分子の会合相互作用を取り込んだ溶液理論の新たな展開を行い，これをもとに疎水性凝集による熱可逆性高分子ゲルの相図の研究を行ってきた [1, 2]．この会合溶液理論では，Flory-Huggins の混合自由エネルギーに反応の自由エネルギーを加えた全自由エネルギーを考察した．最近この溶液理論に高分子のコイル・ヘリックス転移などのコンホメーション転移を取り込み，水素結合系に適用できるように拡張強化した．本書では会合溶液理論を水素結合超分子系に適用して得られたゲルや誘起ヘリックスに関する最近の成果を報告する．(会合溶液理論の詳細は文献 [1, 2] を参照して欲しい.)

2　水素結合超分子液晶の多相臨界性

水素結合の方向性を利用して超分子に液晶相を発現させる試みは，ピリジンとカルボン酸間等の強い水素結合を用いて様々なアーキテクチュアので行われて来た（図 1）．最も単純なタイプは末端に短い剛直部分を有する非液晶性の A 分子と B 分子を水素結合し，複合分子 C=A·B の結合部分がメソゲンとなり液晶を形成する場合である．複合分子は熱的に分解可能であるので，温度変化により等方相からネマチック，スメクチックへと可逆的にかつ重層的に相転移する．実際は，A·B·A 型の複合分子で加藤氏らによって水素結合性液晶が初めて確認された（図 1 の trimer type）[3]．これらの水素結合性液晶分子は，線状に会合させる主鎖型，側鎖にスペーサを経て付ける側鎖型の高分子液晶等に拡張でき，分岐鎖の末端結合の場合のように，無限大の 3 次元連結構造（ネットワーク構造）にまで発展するものもある．

これらの水素結合超分子液晶の相転移を解析するため，会合反応の他にメソゲン間の配向相互作用による自由エネルギーを取り入れた高分子溶液理論にもとづいて，マクロ相分離，ネマチック・スメクチック液晶転移，ゾル・ゲル転移の相境界を導出した．最も典型的な例として，それぞれ個別では液晶にはならないが，2 量体を形成してメソゲンになり，様々な液晶転移を重層的に引き起こすような 2 成分混合系 A/B について得られた相図を図 2 に示す [4].

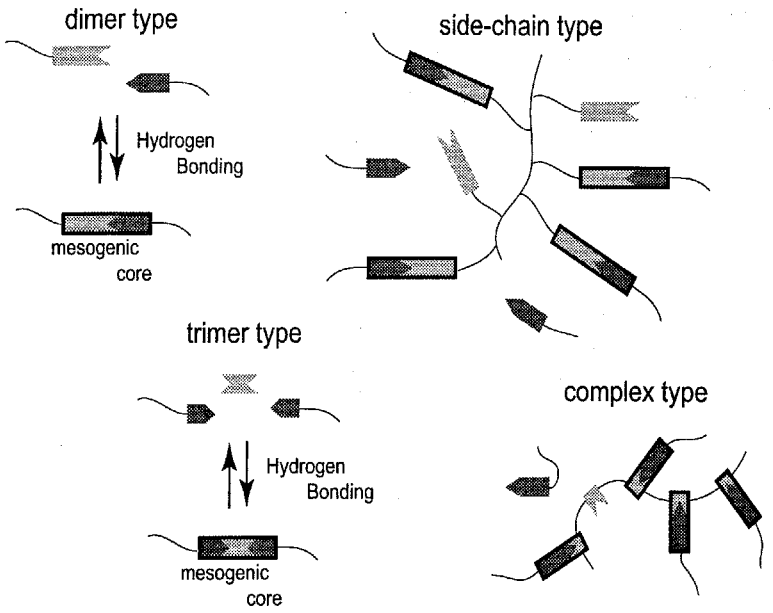

図 1: 種々の水素結合超分子液晶.

この系ではネマチック，スメクチック液晶転移（1 次，2 次相転移いずれも可能）がマクロ相分離（1 次相転移）と競合する．このような 2 つの 1 次相転移のギャップが交叉すると，相分離領域から特徴的な細い 2 相共存領域が高温側に伸び出した相図（「チムニー型相図」と呼ばれる）になる（図 2）.

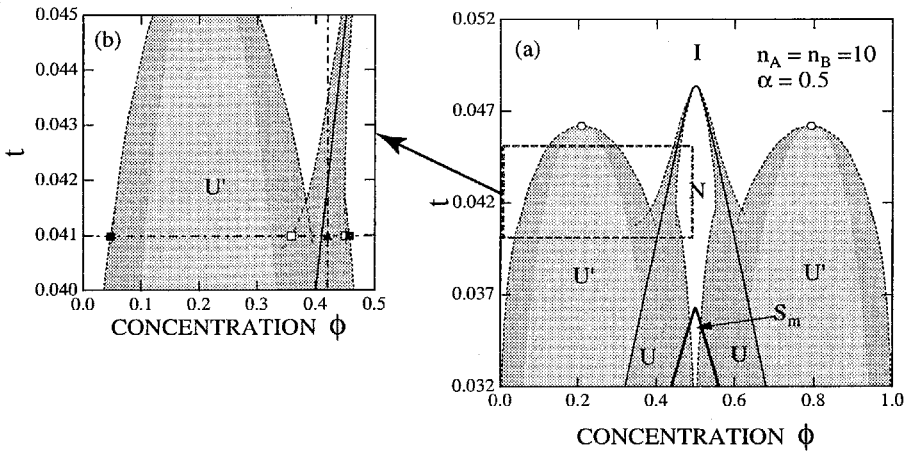

図 2: 水素結合による 2 量体形成の温度-濃度平面での相図.

3 水素結合ヘリックス（ジッパー型）架橋ゲルの再帰ゾル・ゲル転移

水素結合は「一つのボンドが形成されるとその隣接部位に他ボンドが形成されやすくなる」という連鎖性を有している．連鎖性は結合部位の近傍にある未反応基が結合領域に入り易くなることによって生じる．水素結合の連鎖性により特徴的な架橋領域，すなわちジッパー（ファスナー）型の架橋領域を形成するような新しいタイプのゲル（ジッパーゲルと呼ぶ）について，ゾル・ゲル転移の性質，架橋長と

ゲル点との関係，徐冷による架橋領域の成長，弾性率の温度依存性，などを研究した．図3に示すように，天然高分子では水素結合により2重らせんの架橋領域が形成される場合や，はしご（ジッパー）型の架橋領域が形成される場合が多い．また，多糖類が金属イオンを補足してエッグボックス型の細長い架橋領域が形成されるゲルも，ここでジッパーゲルと呼ぶものの一種とみなすことができる．ジッパーゲルの特性を理解するために，しばらくヘッリクス形成について考えよう．

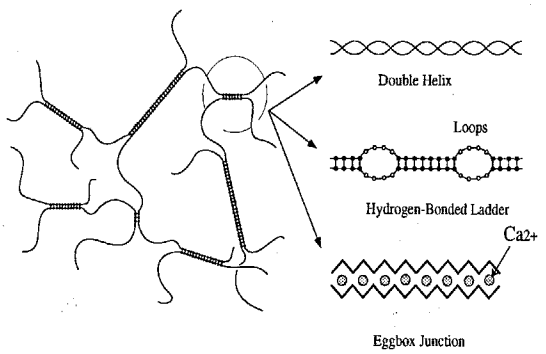

図 3: ジッパー型の架橋構造を持つゲルの生成（上から順に二重らせん，水素結合はしご，イオン補足エッグボックス型）．

単一鎖のヘリックス長の分布関数（べき乗則）については，1960年代のZimmとBraggの理論研究（以下ではZBと略記する）およびそれに続く研究で解明されている[5, 6]．これらの研究では，鎖の分配関数を転送行列の最大固有値から求める方法を使用しているが，この方法は溶液中で相互作用する多鎖の問題には適用できない．高分子鎖の数だけ転送行列を導入しなければならないからである．そこで我々は，単一鎖の問題を組合せ論的に解き直すことから始め，部分ヘリックスの分布関数をもとに，ヘリックス間の会合現象にゲル化のカスケード理論[7, 8]を適用する考えで一連のヘリックスゲルの問題を解析した．今，モノマー数で数えて全長がnの鎖上に長さがζの部分ヘリックスがj_ζ個だけ形成されているとする．単一鎖については分配関数は

$$Z_n(\{j\}) = \sum_{\{j\}} \omega(\{j\}) \prod_{\zeta} (\eta_\zeta)^{j_\zeta} \tag{1}$$

のように表せることに留意する．ここで

$$\omega(\{j\}) \equiv [n - \sum \zeta j_\zeta]! / \left\{ \prod_{\zeta} j_\zeta! [n - \sum (\zeta + 1) j_\zeta]! \right\} \tag{2}$$

はこのような連鎖の分布を限られた総長nから選び出す異なる方法の数，またη_ζはランダムコイル状態を基準にして測った長さζのヘリックスの統計重率である．この重率はZB理論では

$$\eta_\zeta = \sigma s(T)^\zeta \tag{3}$$

の形に仮定されている．ここで$s(T)$はヘリックス中のモノマー1個あたりの水素結合自由エネルギーで表される重率で温度Tの関数であり，体系の温度変化は$s(T)$を通じて表される．またσは最初の1個のモノマーがヘリックスを核生成する確率で，**ヘリックス開始確率**と呼ばれる．さて，分配関数を最大にする最確分布を求めると

$$j_\zeta / n = (1 - \theta - \nu) \eta_\zeta t^\zeta \tag{4}$$

となる．ここで，$\theta \equiv \sum_{\zeta=1}^{n} \zeta j_\zeta/n$ はヘリックスの総量，$\nu \equiv \sum_{\zeta=1}^{n} j_\zeta/n$ はヘリックスの総数である．パラメータ t は方程式

$$tV_0(t)/(1-t) = 1, \qquad (\text{ここで} \quad V_0(t) \equiv \sum_{\zeta=1}^{n} \eta_\zeta t^\zeta) \tag{5}$$

を解いて得られる根である．重率を ZB 型に仮定すると，このようにして求めた θ や ν は ZB の結果 [5] と一致する．

さて，次に多鎖問題，すなわち異なる鎖上のヘリックスの会合現象に移ろう．一般にヘリックスゲルには，単鎖ヘリックスが２重，３重に多重会合する場合と，単鎖ではヘリックスが形成されず，２重鎖，３重鎖ではじめてヘリックスが形成される場合がある．前者では，ランダムコイル状態にある高分子が冷却により様々な長さの短鎖ヘリックスを鎖上に誘起し，これらが一種の会合基として働き架橋が形成される．ゲルのネットワーク中には会合していないヘリックスが残留しているので，ヘリックスの総量とゲルの弾性率が必ずしも比例しない．また，架橋領域に凝集しているヘリックスの長さは均一ではない可能性がある．これに比べて後者では，その定義から必ず２本，３本の鎖が結合していて，孤立している多重鎖というのは存在しない．すなわち，すべてのヘリックスが架橋点となっているので，ヘリックス量とゲルの弾性率とは強い相関がみられる．また，ヘリックスに参加している鎖の連鎖長はすべて等しい．

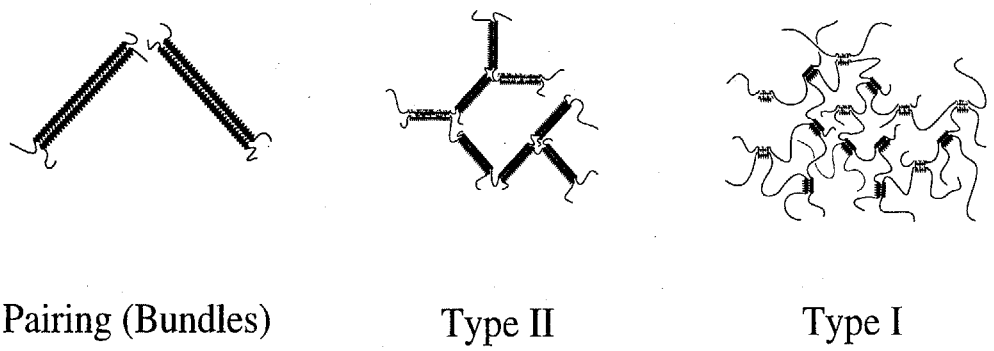

図 4: コイル・ヘリックス転移 による基本的な凝集構造．鎖上に短いヘリクスが多数形成される場合には TypeI のネットワークが形成される．長いヘリックスが少数形成される場合には TypeII のネットワークとなる．TypeII は剛直棒状分子を短鎖ランダムコイルで架橋したネットワークと考えられ，非線形な弾性を有する．ヘリックス長が高分子全長に近くなると，バンドル（ペア）が形成される．

さて，各ヘリックスは一種の官能基とみなすことができるので，ヘリックスの総数は鎖の官能数に該当し，各々の会合強度はヘリックス長に比例するので，以下の２つのメカニズムが競合することが理解される．すなわち，短いヘリックスを多数有する鎖は官能性が高いが凝集エネルギーは低い．逆に，長いヘリックスを少数有する鎖は官能性は低いが凝集エネルギーは大きい．このようにゲルのネットワーク形成に関してはヘリックスの自鎖上での成長と他鎖ヘリックスとの会合とが競合し，いずれが優勢かに従って２つの構造に大別される．このことを単鎖ヘリックスの対会合を例にとって調べてみよう（図 4）．ヘリックス会合が優勢な場合には，各鎖は短いヘリックスを多く有し，ランダムコイルがこれらのヘリックスの凝集により架橋されたネットワクークとなる（TypeI 構造）．逆にヘリックス成長が優勢の場合には，各鎖は長いヘリックスを少数有しているだけなので，ヘリックスペアが短鎖ランダムコイルにより架橋されたネットワークとなる（TypeII 構造）．この場合，ネットワークの部分鎖がヘリックスで，架橋部がランダムコイルと考えるべきである．ヘリックス成長が支配的な極限では，鎖全体が棒状ヘリックスとなるので，ネットワークは形成されず，バンドルが形成される（ペア相）．このような違いは，会合定数に現れる会合エネルギー ϵ_A と，ヘリックス形成に携わる隣接アミノ酸残基間の水素

結合エネルギー ϵ_H の比 $\gamma \equiv \epsilon_A/\epsilon_H$ の値によって区別される．

以上のような考えに基づき，会合強度の異なる会合基がある一定の分布に従って鎖上に出現するような高分子の熱可逆ゲルのモデルを構築し，カスケード理論を使ったゲル化の会合溶液理論によりゾル・ゲル転移について調べた [9]．ヘリックスの分布関数は

$$j_\zeta/n = (1-\theta-\nu)\eta_\zeta u(z_\zeta)t^\zeta \tag{6}$$

となり，単一鎖の (4) 式にヘリックス間の凝集構造を表すカスケード架橋点関数 $u(z)$ が因子としてかかったものになる．パラメータ z_ζ は高分子の体積分率 ϕ と関係 $\lambda(T)j_\zeta\phi/n = z_\zeta u(z_\zeta)$ の関係式で結ばれている．ここで，$\lambda(T)$ は会合定数である．根 t を求める方程式を解き，分布関数を温度 T と高分子濃度 ϕ で表すと，実測可能な物理量を温度，濃度の関数として求めることができる．

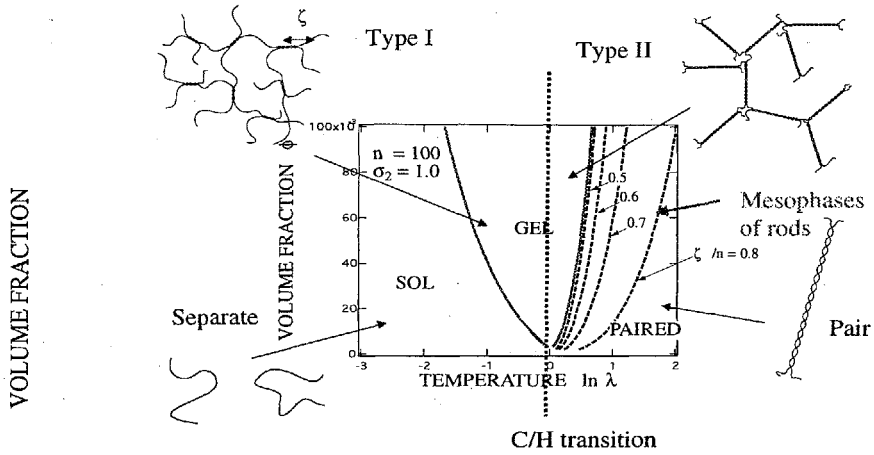

図 5: 2 重鎖ヘリックス架橋ゲルの相図．ゾル・ゲル線（実線）と架橋長の等高線（点線）．

図 5 には，最も興味深い 2 重鎖ヘリックスの場合の相図を温度・濃度平面で示してある．実線はゾル・ゲル転移線，点線はヘリックス長が一定の等高線を表す．低温ではヘリックスが成長することにより，高分子 1 本当たりのヘリックス数が 2 より小さくなり，ネットワーク相からペア相に再帰ゲル・ゾル転移を起こすことがわかる．2 重ヘリックスは剛直棒状分子と考えられるので，ペア相では高濃度領域で種々の液晶が出現したり，棒状分子が互いに集積したレオロジー的なゲル相になったりすることが予測される．ヘリックス量の理論計算はイオタカラギーナン水溶液の旋光度実験データと良好な一致をみた (図 6)．

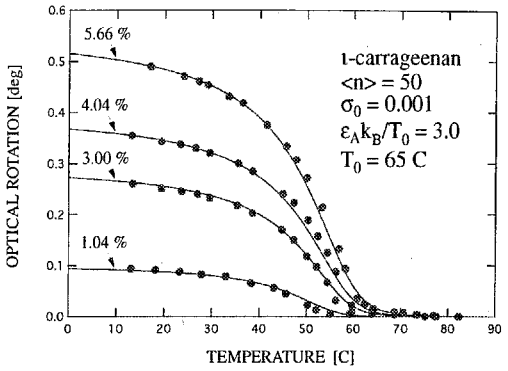

図 6: 2重鎖ヘリックスの総量 θ とイオタカラギーナン希薄溶液の旋光度測定結果との比較.

4 キラル分子による水素結合誘起ヘリックス高分子

水素結合の連鎖性によって発現するヘリックスのもう一つの例を紹介しよう．近年，八島らのグループではキラルな低分子（アミンやアミノアルコール）を高分子（カルボキシフェニルアセチレン）に側鎖基として水素結合させることにより，主鎖の高分子に左右の決まった方向のらせんを誘起する実験を行ってきた [10]．我々はこれらの一連の実験で報告されて来た CD 強度に関するデータと（キラル分子の吸着量に比例する）誘起らせん量の理論計算とを比較検討し，(1) 誘起らせんの非線形増幅現象，(2) 多数支配の法則，(3) 少数指令の法則，について分子論的なメカニズムについて検討した．

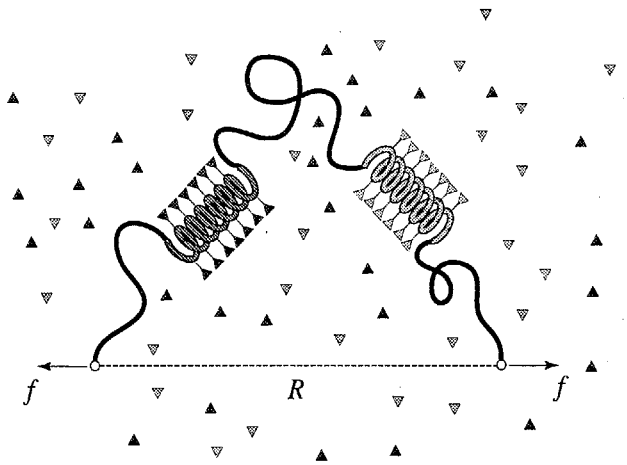

図 7: キラルな低分子の S 体と R 体が混合した溶液中での高分子への水素結合による吸着とらせん誘起現象.

図 7 に示すように，高分子の希薄溶液にキラルな低分子を混合し，低分子がかさ高い側鎖基に水素結合することにより主鎖に捩れが生じ，高分子にらせんが誘起されるものとする．高分子の重合度を n，S 型低分子のモル濃度を $c^{(S)}$，R 型のそれを $c^{(R)}$ とする．希薄溶液なので高分子間の相互作用は考えないことにし，注目した一本鎖のまわりの溶液は一定の化学ポテンシャルを有する低分子の粒子供給源とみなされるものとする．キラリティの偏極度を表すエナンチオマー過剰率は $e \equiv (c^{(S)} - c^{(R)})/(c^{(S)} + c^{(R)})$ で定義される．純粋な S 型（R 型）のみの溶液では $e = 1$（$e = -1$）で，ラセミ溶液の場合は $e = 0$ で

ある．側鎖基はかさ高いので隣り合う吸着分子間には相互作用が生じ，同一キラリティの分子が臨席した場合には主鎖の捩れにより立体的に安定化され連鎖的な吸着が起こるものとする．また，異なるキラリティの分子は立体障害により互いに臨席することができないものとする．このような状況では左右のヘリックスが有限の鎖長の中から自分の席を奪い合うことになるので，媒体中のキラル分子の微小な濃度差が拡大されて現れる．

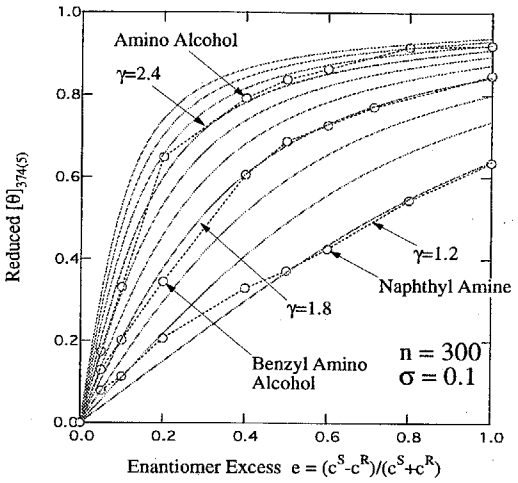

図 8: S, R 型両者が共存する溶液中での吸着曲線．左右のらせん誘起が競合するので全体としてはキラル秩序度 $\psi \equiv \theta^{(S)} - \theta^{(R)}$ が CD 強度に比例する．3 つの低分子アミノアルコール，ベンジルアミノアルコール，ナフチルアミンについてエナンチオマー過剰率の関数として CD 強度とキラル秩序度とをプロットした．微小な過剰率が急激な非線形 CD 誘起に導くいわゆる多数支配の法則（Majority Rule）が読みとれる．全濃度が大きいほどこの効果は著しい．

今，長さ ζ の S 型連鎖が $j_\zeta^{(S)}$ 個，R 型連鎖が $j_\zeta^{(R)}$ 個生じているものとすると，このような連鎖を有限長 n から選び出す方法の数は

$$\omega(\{j\}) = [n - \sum \zeta(j_\zeta^{(S)} + j_\zeta^{(R)})]!/\left\{\prod_\zeta (j_\zeta^{(S)}! j_\zeta^{(R)}!)[n - \sum(\zeta+1)(j_\zeta^{(S)} + j_\zeta^{(R)})]!\right\} \tag{7}$$

で与えられるので，一種ヘリックスの場合の (1) 式を二種ヘリックスの分布関数に場合に拡張し，それぞれ一定の活動度 λ_S，λ_S をもつキラル分子の粒子源の大分配関数を求める．この大分配関数を最大にする最確分布関数を求めると

$$j_\zeta{}^{(\alpha)}/n = (1 - \theta - \nu)\eta_\zeta{}^{(\alpha)}(\lambda_\alpha t)^\zeta \qquad (\alpha = \mathrm{S}, \mathrm{R}) \tag{8}$$

となることが分かる．ここで，$\theta \equiv \theta^{(S)} + \theta^{(S)}$，$\nu \equiv \nu^{(S)} + \nu^{(S)}$ なので，S 体と R 体に対する方程式が連立方程式となっている．これらからヘリックス量がキラル低分子の活動度（濃度）の関数として求められる．図 8 には CD 強度の測定データとヘリックス量の理論計算とを比較した．両者の間の比例定数は未知数であるので，倍数を調節し最適フィットから推定した [11]．このような理論計算を行うことにより，実験では検出の困難な物理量，たとえば，ヘリックスの平均長，高分子鎖あたりのヘリックスの個数（従ってらせん反転の平均数）などが推定され，誘起らせん現象の解析が進むことが期待される．

参考文献

[1] F. Tanaka, *Polym. J.*, **74**, 479 (2002).

[2] F.Tanaka, in *"Molecular Gels"*, ed. by P.Terech and R.G.Weiss, to appear, Kluwer Academic Pub. (2004).

[3] 加藤隆史, 液晶 **4**, 4 (2000).

[4] M.Shoji and F.Tanaka, Macromolecules, **35**, 4760 (2002).

[5] B.H. Zimm and J.K. Bragg, *J. Chem. Phys.*, **31**, 526 (1959).

[6] D. Poland and H.A. Scheraga, *Theory of Helix-Coil Transitions in Biopolymers*; Academic Press (1970).

[7] M.Gordon, *Proc. Roy. Soc. (London)*, **A268**, 240 (1962).

[8] F. Tanaka, *J. Polym. Sci., Part B: Polym. Phys.* , **41**, 2405; 2413 (2003).

[9] F.Tanaka, *Macromolecules*, **36**, 5392 (2003).

[10] E.Yashima, T.Matsushima and Y.Okamoto, *J. Amer. Chem. Soc.*, **119**, 6345 (1997); E.Yashima, K.Maeda and Y.Okamoto, *Nature*, **399**, 449 (1999).

[11] F.Tanaka, *Macromolecules*, **37**, 605 (2004).

＜原著論文・解説＞

1) FumihikoTanaka and Tsuyoshi Koga

Theoretical and Computational Study of Thermoreversible Gelation

Bull. Chem. Soc. Japan, **74**, #2 (2001) 201-215.

2) Fumihiko Tanaka

Theoretical Study of Molecular Association and Thermoreversible Gelation in Polymers

Polymer Journal, **34,** #7 (2002) 479-509.

3) Fumihiko Tanaka

Intramolecular Micelles and Intermolecular Crosslinks in Thermoreversible Gels of Associating Polymers

J. Non-Crystalline Solids, **307-310,** (2002) 688-697.

4) Fumihiko Tanaka

Flows in Polymer Networks

JSME International J, Ser.B **45,** #1 (2002) 123-128

5) Toshio Nakao, Shinzo Kohjiya and Fumihiko Tanaka

Cascade Theory of Substitution Effect in Non-Equilibrium Polycondensation

Macromolecules, **35**, #4 (2003) 5649-5656

6) Masahiko Shoji and Fumihiko Tanaka

Theoretical Study of Hydrogen-Bonded Supramolecular Liquid Crystals

Macromolecules, **35**, #19 (2002) 7460-7472

7) 田中文彦

高分子の会合と相形成に関する理論・シミュレーション

未来材料 **2** #6 (2002) 24-29

8) 田中文彦

高分子の会合による相転移と相図予測

粉体工学会誌 **39** #10 (2002) 25-33

9) Fumihiko Tanaka

Thermoreversible Gelation Driven by Coil-to-Helix Transitions of Polymers

Macromolecules, **36**, #14 (2003) 5392-5405

10) Fumihiko Tanaka

Gel Formation with Multiple Interunit Junctions I

J. Polym. Sci., B: Polymer Physics, **41** (2003) 2405-2412

11) Fumihiko Tanaka

Gel Formation with Multiple Interunit Junctions II

J. Polym. Sci., B: Polymer Physics, **41** (2003) 2412-2421

12) Fumihiko Tanaka

Theoretical Study of Helix Induction on a Polymer Chain by Hydrogen-Bonding Chiral Molecules

Macromolecules, **37**, #2 (2004) 605-613

13) Tsutomu Furuya, Tsuyoshi Koga and Fumihiko Tanaka

Effect of Added Surfactants on Thermoreversible Gelation of Associating Polymer Solutions

J. Polym. Sci., B: Polymer Physics, **42** (2004) 733-751

14) Fumihiko Tanaka

Theory of Molecular Association and Thermoreversible Gelation

Chap.1 in "Molecular Gels" ed. P.Terech and R.G.Weiss,

Kluwer Academic Press (2004) 1-68.

15) Tsutomu Indei and Fumihiko Tanaka

Rheological Study of Transient Polymer Networks Crosslinked by Two-Component Associative Groups

--- Inversion of the Gel Skeletal Structure ---

J. Rheol., In press (2004)

INTERNATIONAL CONFERENCES

[1] Fumihiko Tanaka (invited)

Intramolecular Micelles and Intermolecular Crosslinks in Thermoreversible Gels of Associating Polymers

4th International Discussion Meeting on Relaxation in Complex Systems

18-26 June, 2001

Creta Maris Hotel, Crete, Greece

[2] Fumihiko Tanaka (invited)

Flows in Polymer Networks

The First International Symposium on Advanced Fluid Information (AFI 2001)

4-5 October, 2001

Miyagi Zao Royal Hotel, Sendai, Japan

[3] Tsutomu Furuya and Fumihiko Tanaka

Polymer-Surfactant Interaction in Thermoreversible Gels of Associating Polymers

The First International Symposium on Advanced Fluid Information (AFI 2001)

4-5 October, 2001

Miyagi Zao Royal Hotel, Sendai, Japan

[4] Fumihiko Tanaka (invited)

Thermoreversible Gelation strongly coupled to Polymer Conformational Transition

7th Pacific Polymer Conference

3-7 December, 2001

Hotel Mision de Los Angeles, Oaxaca, Mexico

[5] Fumihiko Tanaka

Thermoreversible Gelation of Associating Polymers

International Symposium on Polymer Physics---PP'2002 Qingdao

2-6 July, 2002

Qingdao, China

] Fumihiko Tanaka

Thermoreversible Gelation induced by Polymer Conformational Transition,

Polymer Networks 2002, Functional Networks and Gels

2-6 September, 2002

Autrans, France

] Fumihiko Tanaka (invited)

Thermoreversible Gelation strongly coupled to the Coil-to-Helix Transition of Polymers,

J"ulich Soft Matter Days 2002,

19-22 November, 2002

Congrescentrum Rolduc, Kerkrade, The Netherlands

| Fumihiko Tanaka (invited)

Thermoreversible Gelation strongly coupled to the Coil-to-Helix Transition of Polymers,

IUMRS-ICAM 2003,"Colloids and Soft Matter",

10-12 October, 2003

Pacifico Yokohama, Yokohama, Japan

| Fumihiko Tanaka

Helix Induction on Polymers by Hydrogen-Bonded Chiral Molecules,

Gordon Conference on Colloidal, Macromolecular and Polyelectrolytes Solutions

1-6 February, 2004

Ventura Beach Marriot, Ventura, California, USA

)] Tsutomu Indei and Fumihiko Tanaka

Transient Network Theory of Co-Associating Polymers ---Molecular Designing and Rheology---,

Gordon Conference on Colloidal, Macromolecular and Polyelectrolytes Solutions

1-6 February, 2004

Ventura Beach Marriot, Ventura, California, USA

REVIEW ARTICLE

Contents

Chapter 1

THEORY OF MOLECULAR ASSOCIATION AND THERMOREVERSIBLE GELATION

Fumihiko Tanaka
Department of Polymer Chemistry
Kyoto University
ftanaka@phys.polym.kyoto-u.ac.jp

Abstract This chapter is devoted to present a general theoretical framework for deriving phase digrams of associating solutions and mixtures. Our theory starts from the conventional lattice-theoretical description of polymer solutions, but incorporate with molecular association and network formation from the viewpoint of chemical equilibrium in bond formation. Applications to the aggregates of low molecular-weight molecules as well as polymers with finite aggregation number are demonstrated, followed by the studies of more complicate infinite aggregates (networks) on the basis of the cascade theory of gelation extended to suit for complex cross-links.

Keywords: Association, Thermoreversible Gelation, Phase Separation, Phase Diagram, Low-Mass Gelator, Hydrogen Bond, Hydrophobic Aggregation, Hydration, Multiple Cross-Link, Micellar Junction, Mixed Network

1. THERMODYNAMIC THEORY OF NETWORK-FORMING LIQUUID MIXTURES

The purpose of this chapter is to present a general theoretical framework for deriving phase diagrams of multicomponent liquid mixtures of low molecular-weight molecules, as well as high molecular weight polymers, in which molecules associate with each other by strongly attractive forces such as hydrogen bonds, hydrophobic force, etc. We treat association from the viewpoint of reversible chemical reactions in forming molec-

ular complexes by such associative forces. We first present a general theory for studying molecular weight distribution function of aggregates and phase transitions induced by association. These transitions include macro- and microphase separation, micellization, hydration, thermoreversible gelation and liquid-crystallization. To stress the unique feature of gelation, we classify the type of association into non-gelling and gelling one. In non-gelling mixtures, oligomers or clusters of finite size are stabilized, while in gelling ones, aggregates grow to macroscopic scales. Theoretical treatment of these two cases is fundamentally different. Several possible applications of the theory to non-gelling systems are presented, followed by the detailed study of thermoreversible gelation with multiple cross-link junctions with special attention to the multiplicity and sequence length of the network junctions. Then, the theory is applied to more complex thermoreversible gels such as binary networks (interpenetrating networks, alternating networks and randomely mixed networks). Potential applications to hydrated networks with high-temperature gelation, to polymer-surfactant interaction etc. are suggested.

1.1 Models of Associating Mixtures

As a model system we consider a binary mixture of linear polymers $\mathrm{R}\{\mathrm{A}_f\}$ and $\mathrm{R}\{\mathrm{B}_g\}$. The number of statistical units on a chain (referred to as degree of polymerization DP) is assumed to be n_A for $\mathrm{R}\{\mathrm{A}_f\}$ chains and n_B for $\mathrm{R}\{\mathrm{B}_g\}$ chains. Although we use a word "polymer" for a primary molecule forming complexes, we may apply our theory to low molecular weight molecules equally well by simply fixing n_A and/or n_B at small values. These polymers are assumed to be reactive and carry a fixed number f of reactive groups indicated by A for $\mathrm{R}\{\mathrm{A}_f\}$ and a number g of reactive groups B for $\mathrm{R}\{\mathrm{B}_g\}$, both capable of forming reversible bonds that can thermally break and recombine. Hydrogen bonds, hydrophobic interaction, electrostatic interaction etc. are important examples of such associative forces. The type of associative interaction does not need to be specified at this stage, but will be detailed in each of the following applications. We symbolically write this model system as $\mathrm{R}\{\mathrm{A}_f\}/\mathrm{R}\{\mathrm{B}_g\}$. In the experiments, various types of solvents are commonly used, so that we should consider a mixture $\mathrm{R}\{\mathrm{A}_f\}/\mathrm{R}\{\mathrm{B}_g\}/\mathrm{S}$, where S denotes a solvent. Extension of the following theoretical consideration to such ternary systems is straightforward. Therefore, for simplicity, we confine in this article to binary systems. Forces working among associative groups form intermolecular clusters covering a wide range of aggregation number. If either of the functionalities f or g exceeds the critical value (3 for pairwise association, but can be 2 for

multiple association), a cluster grows to macroscopic dimensions as soon as a threshold in the temperature, or in the composition (concentration), is reached. Above such a threshold, three-dimensional networks, most generally comprized of the two components, are formed[1, 2, 3, 4, 5].

To describe such reversible network formation in associating mixtures, we take the simplest theoretical view, and start from a conventional lattice theoretical picture of polymer solutions [6, 7, 8, 9] with attempt to include association [10, 11, 12] in the form of reaction equilibrium. Let us first divide the total volume V of the system into small cells of size a of the monomeric unit on a chain [6]. We have total number $\Omega \equiv V/a^3$ of the microscopic cells. We first specify the part of the system containing only clusters of finite size, which will be referred to as *sol*. Let $N_{l,m}$ be the number of connected clusters consisting of the number l of $\mathrm{R}\{\mathrm{A}_f\}$ molecules (referred to as A-chains) and m of $\mathrm{R}\{\mathrm{B}_g\}$ molecules (B-chains). We introduce the symbol (l, m) to specify such a cluster. The total volume fraction of A-chains in the sol is given by

$$\phi_A^S = n_A \sum_{l,m} l\nu_{l,m}, \tag{1.1}$$

where $\nu_{l,m} \equiv N_{l,m}/\Omega$ is the number of clusters per lattice cell. Similarly, the total volume fraction of B-chains in the sol is given by

$$\phi_B^S = n_B \sum_{l,m} m\nu_{l,m}. \tag{1.2}$$

The total volume fraction of the sol in the system is given by $\phi^S = \phi_A^S + \phi_B^S$. This should be equal to unity for nongelling systems, or in the *pregel regime* of gelling systems, but can be smaller than unity as soon as an infinite network (referred to as *gel*) appears, i.e., in the *postgel regime* of the gelling systems. In the postgel regime, the volume fraction of the chains of species i in the gel network is given by $\phi_i^G = \phi_i - \phi_i^S$ for i =A,B, where ϕ_i is the total volume fraction of the species i that is fixed at the preparatory stage of the experiments. The number density ν_i^G of the species i in the gel is then given by $\nu_i^G \equiv \phi_i^G/n_i = N_i^G/\Omega$ for i =A,B, where N_i^G is the number of i-chains in the gel. Such decomposition into the sol part and the gel part automatically takes place in accordance with the thermodynamic principles. Since we have an identity $\phi_A + \phi_B = 1$, in what follows we can take ϕ_A as an independent variable and write it simply as ϕ. The volume fraction of B is then given by $\phi_B = 1 - \phi$.

1.2 Free Energy and Distribution Function of Aggregates

In order to study thermodynamic properties, we start from the *standard reference state* in which unconnected A-chains and B-chains are prepared separately in a hypothetical crystalline state [6, 8]. We first consider the free energy change ΔF_{rea} to bring the system from the reference state to a fictitious intermediate state in which chains are disoriented and connected in such a way that the cluster distribution is exactly the same as the real one [12, 13, 14]. It is given by

$$\beta\Delta F_{rea}/\Omega = \sum_{l,m} \Delta_{l,m}\nu_{l,m} + \delta_A\nu_A^G + \delta_B\nu_B^G, \tag{1.3}$$

where $\Delta_{l,m}$ is the free energy produced when a single (l,m) cluster is formed from l of A-chains and m of B-chains in the reference state. We call this *free energy of reaction.* Let $\mu^\circ_{l,m}$ be the internal free energy of an (l,m) cluster. The free energy difference $\Delta_{l,m}$ is then given by

$$\Delta_{l,m} = \beta(\mu^\circ_{l,m} - l\mu^\circ_{1,0} - m\mu^\circ_{0,1}). \tag{1.4}$$

Under a constant pressure, $\mu^\circ_{l,m}$ is equivalent to the internal free energy produced by combination, configurational change, and bond formation of the constitutional primary molecules. Specific forms of these contributions will be considered in each problem we study in the following. Similarly, δ_i (i =A,B) show the free energy change produced when an isolated chain of the species i is connected to the gel network. They are given by $\delta_A = \beta(\mu_A^{\circ G} - \mu^\circ_{1,0})$ and $\delta_B = \beta(\mu_B^{\circ G} - \mu^\circ_{0,1})$, where $\mu_i^{\circ G}$ is the internal free energy of an i-chain in the gel network. The two last terms in eq.(1.3) are necessary in the postgel regime because the number of molecules contained in the gel part becomes macroscopic and reaches a finite fraction of the total number of molecules in the system. In the second step, we mix these clusters with each other to get to a real mixture we study. According to the conventional lattice theory of polydisperse polymer mixtures [8, 9], the mixing free energy ΔF_{mix} in this process is given by

$$\beta\Delta F_{mix}/\Omega = \sum_{l,m} \nu_{l,m} \ln \phi_{l,m} + \chi\phi(1-\phi), \tag{1.5}$$

where $\phi_{l,m} \equiv (n_A l + n_B m)\nu_{l,m}$ is the volume fraction occupied by the (l,m)-clusters, and χ is Flory's χ-parameter which specifies the strength of van der Waals type contact interaction between monomers of different species. The first term gives the mixing entropy of the clusters. Since clusters formed by association are generally polydisperse, and have largely different volumes, mixing entropy of the Flory-Huggins

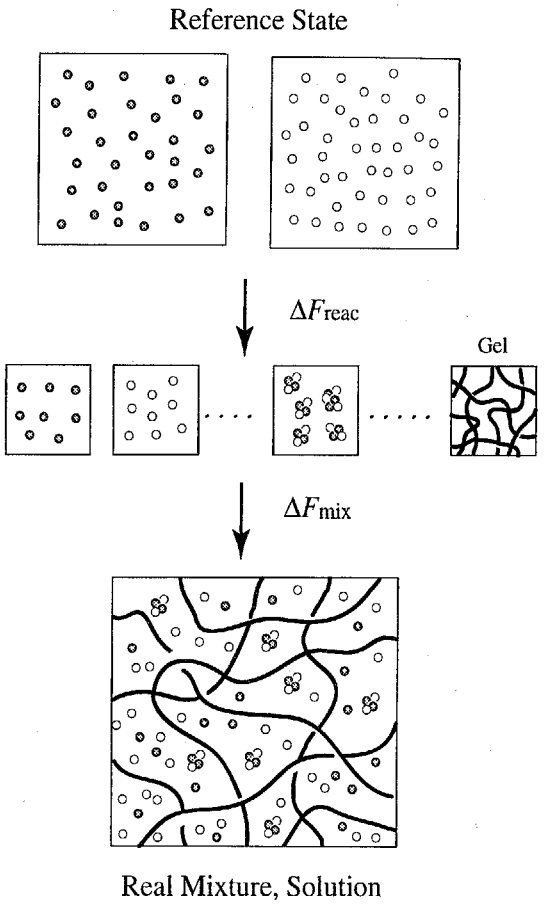

Figure 1.1. Construction of the free energy of associating mixtures. The total free energy is given by the sum of the free energy of reaction and that of mixing. The standard reference state is chosen in such a way that each species of molecules are regularly placed on a hypothetical crystalline lattice with reference intramolecular conformation (straight rod in the case of polymers).

type must be used even if the primary molecules are low molecular-weight molecules. The macroscopically connected clusters such as gel networks, infinitely long linear aggregates do not give the mixing entropy since their centers of mass lose translatonal degree of freedom. The χ-parameter varies with the temperature, but is assumed to be independent of the composition as in the conventional theory. The number of contact between the two species may change by molecular association, and hence the mixing enthalpy (the last term of eq.(1.5)) may be modi-

fied. We assume here, however, that the same form remains valid after association except when the modification is significant due to polymer conformational change etc. We improve this term whenever necessary. The total free energy from which our theory starts is given by the sum of the above two parts:

$$\Delta F = \Delta F_{rea} + \Delta F_{mix}. \tag{1.6}$$

We next derive the chemical potentials of the clusters to study solution properties. By the thermodynamic definition of the chemical potential $\Delta\mu_{lm} \equiv (\partial\Delta F/\partial N_{lm})_{T,N_{l'm'}...}$ for clusters of the size (l,m), we find

$$\begin{aligned}\beta\Delta\mu_{lm} &= 1+\Delta_{lm}+\ln\phi_{lm}-(n_A l+n_B m)\nu^S \\ &\quad +\chi\{n_A l(1-\phi)+n_B m\phi-(n_A l+n_B m)\phi(1-\phi)\} \\ &\quad +[n_A l(1-\phi)-n_B m\phi][\delta'_A(\phi)\nu_A^G-\delta'_B(\phi)\nu_G^B],\end{aligned} \tag{1.7}$$

where

$$\nu^S \equiv \sum_{l,m}\nu_{lm} \tag{1.8}$$

is the total number of finite clusters (per lattice cell) in the mixture. This number gives the total number of molecules and clusters that possess translational degree of freedom. Within ideal solution approximation, they equally contribute to the osmotic pressure. Obviously, gel part is excluded from ν^S because it is macroscopic, and its center of mass is localized. The ratio defined by

$$P_{\rm n} \equiv [\phi/n_A+(1-\phi)/n_B]/\nu^S \tag{1.9}$$

gives the *number-average cluster size*, or *number-average aggregation number* of clusters.

In particular, we have for molecules that remain unassociated

$$\frac{\beta\Delta\mu_{10}}{n_A} = \frac{1+\ln\phi_{10}}{n_A}-\nu^S+\chi(1-\phi)^2+\left[\delta'_A(\phi)\nu_A^G-\delta'_B(\phi)\nu_B^G\right](1-\phi), \tag{1.10a}$$

$$\frac{\beta\Delta\mu_{01}}{n_B} = \frac{1+\ln\phi_{01}}{n_B}-\nu^S+\chi\phi^2-\left[\delta'_A(\phi)\nu_A^G-\delta'_B(\phi)\nu_B^G\right]\phi. \tag{1.10b}$$

Similarly, chemical potentials of the polymer chains in the gel part are given by

$$\beta\Delta\mu_A^G/n_A = \delta_A/n_A-\nu^S+\chi(1-\phi)^2+(1-\phi)\left[\delta'_A(\phi)\nu_A^G-\delta'_B(\phi)\nu_B^G\right] \tag{1.11a}$$

$$\beta\Delta\mu_B^G/n_B = \delta_B/n_B-\nu^S+\chi\phi^2-\phi\left[\delta'_A(\phi)\nu_A^G-\delta'_B(\phi)\nu_B^G\right]. \tag{1.11b}$$

To find the equilibrium distribution of clusters, we impose *multiple chemical equilibrium conditions*

$$\Delta\mu_{l,m} = l\Delta\mu_{1,0} + m\Delta\mu_{0,1} \tag{1.12}$$

for all possible combinations of the integers (l, m). Upon substitution of the specific forms of the chemical potentials, we find that the volume fractions of the clusters are given by

$$\phi_{l,m} = K_{l,m}x^l y^m, \tag{1.13}$$

where for simplicity we have written as x and y for the concentrations $\phi_{1,0}$ and $\phi_{0,1}$ of unassociated molecules. These unassociated molecules in the solution are sometimes called *unimers* to avoid confusion with monomers. The new constant $K_{l,m}$ (*equilibrium constant*) is defined by

$$K_{l,m} \equiv \exp(l + m - 1 - \Delta_{l,m}), \tag{1.14}$$

which depends only on the temperature through $\Delta_{l,m}$. Similarly, the number density of clusters is given by

$$\nu_{l,m} = \frac{K_{l,m}}{n_A l + n_B m} x^l y^m. \tag{1.15}$$

The total volume fraction ϕ^S and the total number ν^S of clusters in the sol part as functions of x and y are then found by the infinite sum:

$$\phi^S(x, y) = \sum_{l,m} K_{l,m}x^l y^m, \tag{1.16}$$

and

$$\nu^S(x, y) = \sum_{l,m} \frac{K_{l,m}}{n_A l + n_B m} x^l y^m. \tag{1.17}$$

1.2.1 Pregel Regime. In non-gelling mixtures, or pregel regime of gelling ones, the total volume fraction should be given by

$$\phi^S(x, y) = 1 \tag{1.18}$$

since all clusters are included in the summation. The volume fraction of each species is then given by

$$\phi = n_A \sum_{l,m} l\nu_{l,m} \tag{1.19a}$$

$$1 - \phi = n_B \sum_{l,m} m\nu_{l,m}. \tag{1.19b}$$

These equations are transformed into the coupled equations

$$\phi = n_A x \frac{\partial \nu^S}{\partial x} \tag{1.20a}$$

$$1-\phi = n_B y \frac{\partial \nu^S}{\partial y} \tag{1.20b}$$

for unknown variables x and y. We solve them with respect to x and y, and substitute the result into the physical quantities we concern. For instance, the number-average number of A-chains and B-chains in the finite clusters are given by

$$< l >_{\rm n} = \frac{\partial \ln \nu^S(x,y)}{\partial \ln x} \text{ and } < m >_{\rm n} = \frac{\partial \ln \nu^S(x,y)}{\partial \ln y}, \tag{1.21}$$

where the average symbol

$$< Q_{l,m} >_{\rm n} \equiv \frac{\sum Q_{l,m}\nu_{lm}}{\sum \nu_{lm}} \tag{1.22}$$

shows the number average of the quantity $Q_{l,m}$. Similarly, the weight-average is defined by

$$< Q_{l,m} >_{\rm w} \equiv \frac{\sum Q_{l,m}\phi_{lm}}{\sum \phi_{lm}}. \tag{1.23}$$

The weight-average of the aggregation numbers l and m in the clusters are then given by

$$< l >_{\rm w} = \frac{\partial \ln \phi^S(x,y)}{\partial \ln x} \text{ and } < m >_{\rm w} = \frac{\partial \ln \phi^S(x,y)}{\partial \ln y}. \tag{1.24}$$

The weight-average DP of the clusters is thus given by the sum

$$\begin{aligned} \overline{M}_{\rm w} &\equiv \frac{\sum (n_A l + n_B m)\phi_{lm}}{\sum \phi_{lm}} = n_A < l >_{\rm w} + n_B < m >_{\rm w} \\ &= \left(n_A \frac{\partial}{\partial \ln x} + n_B \frac{\partial}{\partial \ln y} \right) \ln \phi^S(x,y) \end{aligned} \tag{1.25}$$

1.2.2 Sol/Gel Transition and Postgel Regime. So far we have tacitly assumed that the infinite double summation in ϕ^S (and hence in ν^S) converges. These are double power series with positive coefficients, so that they are monotonically increasing functions. For mixtures capable of gelling, a borderline exists which separates the unit square on the (x,y) plane into a convergent region and a divergent one.

Exactly on the boundary line, the sol composition ϕ^S takes a finite value, but it diverges outside this line. Since the radius of convergence generally depends on the composition, let us express the boundary by a parametric form $(x^*(\phi), y^*(\phi))$ for $0 \leq \phi \leq 1$. The value $\phi^S(x^*, y^*)$ can become smaller than unity for a certain region of the composition and the temperature because the sum *does not include* contributions from the infinite clusters appearing in the postgel regime. Hence we can find the sol/gel transition line by mapping the condition $\phi^S(x^*, y^*) = 1$ onto the original temperature-concentration plane.

In the postgel regime, a chain participating in the gel network must be in chemical equilibrium with an unassociated chain of the same species. This imposes the additional conditions

$$\Delta\mu_{1,0} = \Delta\mu_A^G \quad \text{and} \quad \Delta\mu_{0,1} = \Delta\mu_B^G, \tag{1.26}$$

and hence we find that x and y become functions of the concentration in the form

$$x^* = \exp[\delta_A(\phi) - 1] \quad \text{and} \quad y^* = \exp[\delta_B(\phi) - 1], \tag{1.27}$$

for the gelling component in the postgel regime. Asterisks indicate that they refer to the quatities after the gel point. The chemical potential of each species takes a uniform value in the solution, so that we can write them as $\Delta\mu_A$ and $\Delta\mu_B$.

We now substitute all relations obtained by such equilibrium conditions back into the original free energy (1.6), or equivalently, we use Gibbs-Dühem relation $\Delta F/\Omega = \Delta\mu_A\phi/n_A + \Delta\mu_B(1-\phi)/n_B$, and find the free energy is simply given by

$$\beta\Delta F/\Omega = \frac{1+\ln x}{n_A}\phi + \frac{1+\ln y}{n_B}(1-\phi) - \nu^S + \chi\phi(1-\phi). \tag{1.28}$$

(The concentration x and y should be replaced by x^* and y^* in the postgel regime.) This free energy can be decomposed into two parts as

$$\beta\Delta F/\Omega = f_{\rm FH}(\phi) + f_{\rm AS}(\phi), \tag{1.29}$$

where

$$f_{\rm FH}(\phi) \equiv \frac{\phi}{n_A}\ln\phi + \frac{(1-\phi)}{n_B}\ln(1-\phi) + \chi\phi(1-\phi) \tag{1.30}$$

is the conventional Flory-Huggins free energy of the non-associative counterpart, and

$$f_{\rm AS}(\phi) \equiv \frac{\phi}{n_A}\ln(\frac{x}{\phi}) + \frac{1-\phi}{n_B}\ln(\frac{y}{1-\phi}) + \frac{\phi}{n_A} + \frac{1-\phi}{n_B} - \nu^S \tag{1.31}$$

gives the effect of association. The effect of association can also be regarded as a *renormalization* of the Flory's χ-parameter. It produces the shift from χ to $\chi + \Delta\chi$, where

$$\Delta\chi \equiv f_{\rm AS}(\phi)/\phi(1-\phi). \tag{1.32}$$

The short-range associative interaction energy originally introduced in the reaction terms is now interpreted as a composition-dependent modification of the χ-parameter.

1.3 Phase Separation, Stability Limit and Other Solution Properties

Let us now find some important physical quatities characterizing the mixture.

(1) *Osmotic Pressure* The osmotic pressure π of the A component is essentially the chemical potential of the B species with opposite sign, and given by

$$\beta\pi/n_B a^3 = -(1+\ln y)/n_B + \nu^S(x,y) - \chi\phi^2 + [\delta'_A(\phi)\nu_A^G - \delta'_B(\phi)\nu_B^G]\phi. \tag{1.33}$$

In a polymer solution in which B component is a low molecular weight non-associative solvent ($n_B = 1$ and $\delta_B(\phi) = 0$), this definition reduces to the osmotic pressure in the conventional meaning. If we expand this pressure in powers of the concentration with $n_B = 1$, we have the virial series

$$\pi a^3/k_B T = \phi/n_A + A_2\phi^2 + A_3\phi^3 + \cdots, \tag{1.34}$$

where $A_2 = 1/2 - \chi - \Delta A_2$ with ΔA_2 being a positive temperature-dependent constant. Hence, the second virial coefficient has a reduction ΔA_2 from $1/2-\chi$ due to the associative interaction. At higher concentration across the gel point, the osmotic compressibility $K_T \equiv (\partial\phi/\partial\pi)_T/\phi$, or its higher derivatives, may have discontinuity due to the appearance of the gel part.

(2) *Phase Separation* The two-phase equilibrium conditions, or a *binodal* lines can be found by balancing the chemical potential of each component [8, 9]:

$$\Delta\mu_A(\phi', T) = \Delta\mu_A(\phi'', T), \tag{1.35}$$

$$\Delta\mu_B(\phi', T) = \Delta\mu_B(\phi'', T), \tag{1.36}$$

where ϕ' and ϕ'' are the composition of the dilute A phase and concentrated A phase respectively. If either phase, or both of them, lies inside the postgel regime, chemical potentials must be replaced by their postgel forms $\Delta\mu_A^*(\phi'', T)$ and $\Delta\mu_B^*(\phi'', T)$.

(3) *Stability Limit* The thermodynamic stability limit, or a *spinodal* line, can be found for the binary system by a single condition $(\partial\Delta\mu_A/\partial\phi)_T = 0$, or equivalently, $\partial(\Delta\mu_A/n_A - \Delta\mu_B/n_B)/\partial\phi = 0$. We have the equation

$$\frac{\kappa_A(\phi)}{n_A\phi} + \frac{\kappa_B(\phi)}{n_B(1-\phi)} - 2\chi = 0, \tag{1.37}$$

where the new functions are defined by

$$\kappa_A(\phi) \equiv \phi\frac{d}{d\phi}\left(1 + \phi_A^G\frac{d}{d\phi}\right)\ln x, \tag{1.38a}$$

$$\kappa_B(\phi) \equiv -(1-\phi)\frac{d}{d\phi}\left(1 - \phi_B^G\frac{d}{d\phi}\right)\ln y. \tag{1.38b}$$

In the pregel regime, these equations are related to the weight-average aggregation number of clusters. For homopolymer association where only A-chains are associated, for instance, κ_A reduces to the reciprocal of the weight-average cluster size as in the conventional polydisperse polymer solutions [9, 15]. In heteropolymer association, however, κ's are related to the average cluster sizes in a more complicated way.

2. SOME IMPORTANT EXAMPLES OF NON-GELLING ASSOCIATING MIXTURES

We first show some of the important results obtained so far for the non-gelling mixtures. Throughout this section, we assume pairwise association of reactive groups. The strength of association can be expressed in terms of the three *association constants* defined by

$$\lambda_{AA} \equiv \exp(-\beta\Delta f_{AA}), \quad \lambda_{BB} \equiv \exp(-\beta\Delta f_{BB}), \quad \lambda_{AB} \equiv \exp(-\beta\Delta f_{AB}), \tag{2.1}$$

for three combination of pairs [16], where Δf is the free energy changes on forming a bond of the specified pair. To prevent gelation, we assume that the functionalities of either or both species of polymers are less than or equal to two in this section.

We apply our general theory presented above, and summarize the main results in the form of phase diagrams. For the numerical calculation we introduce the reduced temperature deviation

$$\tau \equiv 1 - \Theta/T \tag{2.2}$$

from the unperturbed theta temperature Θ, which is defined by the equation $\chi(\Theta) = 1/2n_B$. The unrenormalized second virial coefficient

of the osmotic pressure in the generalized sense defined for eq.(1.34) vanishes at this temperature. We then assume Shultz-Flory's form [8, 17]

$$\chi(T) = 1/2n_B - \psi_1\tau \tag{2.3}$$

for the *bare* interaction parameter, where ψ_1 is a dimensionless material parameter of order unity. Since the binding free energy can be split into energy part and entropy one as $\Delta f = \Delta\epsilon - T\Delta s$ for all pairs, we rewrite the association constant $\lambda(T)$ as

$$\lambda(T) = \lambda_0 \exp[\gamma(1-\tau)] \tag{2.4}$$

with the dimensionless binding energy

$$\gamma \equiv |\Delta\epsilon|/k_B\Theta \tag{2.5}$$

and the entropy-related constant $\lambda_0 \equiv \exp(\Delta s/k_B)$ [10, 12].

2.1 Dimer Formation

The first system we study is a mixture of R{A_1} and R{B_1} chains, each carrying a functional group A or B at its one end. Diblock copolymers are formed by the end-to-end association (*hetero-dimerization*) [18]. End groups A and B are assumed to be capable of forming pairwise bond A·B by thermoreversible hetero-association. Hydrogen bond between acid and base pair is the most important example of this category. For such mixtures we have $f = g = 1$. A composite chain formed is a diblock copolymer R{A_1}-*block*-R{B_1} with a temporal junction (Figure 1.2). The system is made up of a mixture of diblock copolymers (1,1), and unassociated homopolymers of each species (1,0) and (0,1). It is apparently the same as a mixture of chemically connected diblock copolymers dissolved in their homopolymer counterparts [19, 20], but its phase behavior is much richer because the population of the block copolymers varies by the change of the temperature and the composition. Let $n \equiv n_A + n_B$ be the total number of the statistical units on a block copolymer chain, and let $a \equiv n_A/n$ ($b \equiv n_B/n$) be the fraction of A part (B part). The relation $a+b = 1$ holds by definition. Our starting free energy is given by

$$\beta\Delta F/\Omega = \Delta\cdot\nu_{11} + \nu_{10}\ln\phi_{10} + \nu_{01}\ln\phi_{01} + \nu_{11}\ln\phi_{11} + \chi\phi(1-\phi), \tag{2.6}$$

where $\Delta \equiv \beta(\mu^\circ_{A\cdot B} - \mu^\circ_A - \mu^\circ_B)$ is the free energy of dimer formation. By diferentiation we find for the chemical potential of each component as

$$\beta\Delta\mu_{10} = \ln x + 1 - n_A\nu^S + \chi n_A(1-\phi)^2, \tag{2.7a}$$

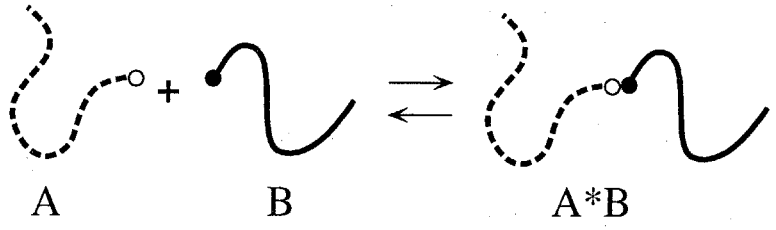

Figure 1.2. Block copolymer formed by reversible association of the pair of end-functional polymers R{A_1} and R{B_1}. The system becomes a mixture of block copolymers R{A_1}-block-R{B_1} and their homopolymers whose population distribution is thermally controlled.

$$\beta\Delta\mu_{01} = \ln y + 1 - n_B\nu^S + \chi n_B\phi^2, \tag{2.7b}$$
$$\beta\Delta\mu_{11} = \Delta + \ln z + 1 - n\nu^S + \chi\{n_A(1-\phi)^2 + n_B\phi^2\}, \tag{2.7c}$$

where $\nu^S \equiv \nu_{10} + \nu_{01} + \nu_{11}$ is the total number of molecules that possess translational degree of freedom, and $x \equiv \phi_{1,0}, y \equiv \phi_{0,1}$, $z \equiv \phi_{1,1}$.

The association equilibrium condition (1.12) then leads to

$$z = Kxy \tag{2.8}$$

for the volume fraction z of the block copolymers, where $K \equiv \exp(1-\Delta)$ is the temperature-dependent association constant. Because of the non-gelling nature, we have an identity

$$\phi^S = x + y + Kxy \equiv 1. \tag{2.9}$$

The number density of clusters is given by

$$\nu^S = \nu = \frac{1}{n}\left(\frac{x}{a} + \frac{y}{b} + Kxy\right). \tag{2.10}$$

Solving the coupled equation (1.20), we find

$$x(\phi) = \{\phi - a - K^{-1} + \sqrt{D(\phi)}\}/2b, \tag{2.11a}$$
$$y(\phi) = \{a - \phi - K^{-1} + \sqrt{D(\phi)}\}/2a, \tag{2.11b}$$

where $D(\phi) \equiv [a(1-\phi) + b\phi + K^{-1}]^2 - 4ab\phi(1-\phi)$.

We now split Δ into the conformation part and bonding part as $\Delta = \beta\Delta f_{\rm conf} + \beta\Delta f_{\rm bond}$. The conformational free energy appears because the entropy of disorientation is reduced when two chains are combined. If we use lattice-theoretical entropy of disorientation [6, 8]

$$S_{\rm dis}(n) = k_B \ln\left\{\frac{n\zeta(\zeta-1)^{n-2}}{\sigma e^{n-1}}\right\} \tag{2.12}$$

for a linear chain of n statistical units (ζ being the lattice coordination number, σ the symmetry factor), we have

$$\Delta S_{\rm dis} \equiv S_{\rm dis}(n_A + n_B) - S_{\rm dis}(n_A) - S_{\rm dis}(n_B) = k_B \ln \left\{ \frac{\sigma(\zeta-1)^2}{\zeta enab} \right\} \tag{2.13}$$

for the entropy change, and the free energy is given by $\Delta f_{\rm conf} = -T\Delta S_{\rm dis}$. Combining the free energy of bonding $\Delta f_{\rm bond} = \Delta\epsilon - T\Delta s$, we find that the equilibrium constant is given by $K = \lambda_0 e^{-\beta\Delta\epsilon}$, where $\lambda_0 \equiv \sigma(\zeta-1)^2 e^{\Delta s/k_B}/\zeta enab$ is a temperature independent constant. The volume fraction of the diblock copolymers z can then be calculated along the general theoretical scheme given above.

It is well known that diblock copolymers form a variety of microscopically ordered phases [21, 22]. To study such microphase separation transitions (MST), one should calculate the correlation function $S(\mathbf{q})$ of the concentration fluctuation as a function of the wave vector $\mathbf{q}$ (and temperature, concentration). Details of the calculation by using random phase approximation can be found in the references [21, 22]. When it is divergent at certain finite wave number q, it is the precursor of the instability against the fluctuation whose spatial variations are characterized by the length q^{-1}—hence leading to the formation of an ordered state with the periodicity q^{-1}. In the case of block copolymers, q^{-1} is of the order of the radius of gyration of a single polymer chain. Divergence of $S(\mathbf{q})$ thus suggests the periodic microdomain formation. We can therefore find MST boundary by the condition

$$S(\mathbf{q})^{-1} = 0. \tag{2.14}$$

From the same standpoint, macroscopic stability limit (or spinodal condition) can also be found from the condition $S^{-1}(\mathbf{q}=0) = 0$ by using the same scattering function. This condition is equivalent to the divergence condition (1.37) of the osmotic compressibility. We applied the general theoretical scheme developed by Leibler [21] and calculated the correlation function [18] for the associating diblock mixture and found the MST boundaries for thermoreversible dimers.

Figure 1.3 shows theoretical calculation of the phase diagram for a symmetric blend where both chains have the same length [18]. Solid lines show the binodal, the broken line shows MST line, and dotted lines the spinodal. MST and spinodal meet at the two symmetric points (indicated by LP) at which the two conditions (1.37) and (2.14) reduces to a single one. They are examples of the *Lifshitz point* — the point where an order parameter with finite wave number starts to appear [19, 23].

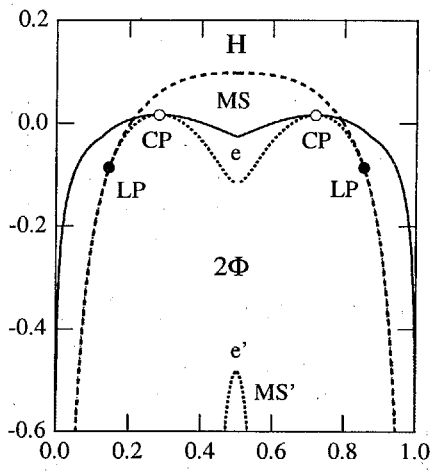

Figure 1.3. A typical phase diagram of associating diblock copolymers in which macro- and microphase separation compete. Binodal (solid line), spinodal (dotted line) and MST(broken line) are drawn. Critical points are indicated by CP. At the crossing of spinodal and MST line, Lifshitz points(LP) appear. At the stoichiometric composition where the number of A groups equals that of B groups, an eutectic point (e) appears. (Reprinted with permission from Ref.[14]. Copyright 2002, Jap. Soc. Polym. Sci.)

The whole plane is divided into several regions, each characterized by the capital letters in it. The region with letter H has a homogeneously mixed fluid phase. Those shown by MS and MS' exhibit microscopically ordered phases where microdomains are regularly ordered. A region with the letters 2Φ in the figure is a biphasic region (or *miscibility gap*) where two distinct phases coexist. The point indicated by the letter e in the middle of the phase diagram is an *eutectic point* where single microphase melt into the two coexisting homogeneously mixed fluids when the temperature is lowered. At extremely low temperature, we observe that the miscibility gap starts to split again at the point e' in the center of the concentration axis, and a new homogeneous microphase (shown by MS') is stabilized in between. Such a low-temperature microphase (called *reentrant microphase*) is stabilized simply because the population of block copolymers becomes so large in this low-temperature region that they homogenize the two demixed fluid phases into a single one.

Experimentally, hydrogen bonds are expected to lead to thermoreversible MST if it is strong enough compared to the repulsive interac-

tion between the polymer segments but still weak enough to break by temperature. In this respect, single hydrogen bond is not strong enough, but through elaborate effort [24, 25, 26] reversible lamellar formation was confirmed to be possible for semi-crystalline block copolymers, i.e., blend of one-end-aminated polystyrene and one-end-carboxylated polyethylene glycol. In contrast, a variety of liquid-crystalline ordered phases induced by *multiple hydrogen bonds* have been a focus of recent research interest [27, 28, 29].

2.2 Linear Association and Ring Formation

In this section, we consider association of polymers R{A_2} carrying two functional groups at their ends (*telechelic polymers*) in a solution. We here confine pairwise association, so that polymers R{A_2} form either linear chains or rings (*Chain/Ring Equilibrium*) [30]. In the case of low-mass gelator[38] carrying two complementary hydrogen-bonding groups, the molecular weight n_A should be a small number, and there is no ring formation due to the stiffness of fibrous aggregates. More general case of multiple association, where polymer networks with micellar junctions are formed, will be treated as a gelling case later. Let N_m^C be the number of m-mer open chains, and let N_m^R be the number of m-mer rings in the system. The total number of primary polymer chains ($n_A \equiv n$) is then given by

$$N = \sum_{m=1}^{\infty} m(N_m^C + N_m^R). \tag{2.15}$$

Let N_0 be the number of solvent molecules ($n_B \equiv 1$). The number of cells is $\Omega = N_0 + nN$. Let $\phi_m^C \equiv nmN_m^C/\Omega$ and $\phi_m^R \equiv nmN_m^R/\Omega$ be the volume fraction of chains and rings. The volume fraction of polymers is then given by

$$\phi = \sum_{m=1}^{\infty} (\phi_m^C + \phi_m^R) = 1 - \phi_0, \tag{2.16}$$

where ϕ_0 is the volume fraction of the solvent. The fraction of rings among the total polymers is given by

$$\rho \equiv \sum_{m=1}^{\infty} \phi_m^R/\phi. \tag{2.17}$$

We follow the general strategy given above, and start with the free energy of the solution

$$\beta\Delta F = \sum_{m\geq 1} \left\{\Delta_m^C N_m^C + \Delta_m^R N_m^R\right\} \tag{2.18}$$

$$+ \quad N_0 \ln \phi_0 + \sum_{m\geq 1} \left\{ N_m^C \ln \phi_m^C + N_m^R \ln \phi_m^R \right\} + \chi\phi(1-\phi)\Omega,$$

where Δ are free energies of reaction defined by

$$\Delta_m^C \equiv \beta(\mu_m^{C\circ} - m\mu_1^\circ) \tag{2.19}$$

$$\Delta_m^R \equiv \beta(\mu_m^{R\circ} - m\mu_1^\circ) \tag{2.20}$$

for chains and rings measured from those of the primary polymers.

We first consider open chains. The number of different ways to connect m identical polymers into a linear array is given by 2^m, but since the connected chain is symmetric, we have to divide it by the symmetry number $\sigma_C = 2$, and hence we have 2^{m-1} for the combinatorial factor. The conformational term is given by the difference $\Delta S_{\rm conf}(m) = S_{\rm dis}(mn) - mS_{\rm dis}(n)$ as before. The bonding free energy is assumed to be given by Δf_0 for each bond. Hence we find

$$K_m^C = 2^{m-1} m \left[\frac{\sigma_C(\zeta-1)^2}{n\zeta} \right]^{m-1} (e^{-\beta\Delta f_0})^{m-1} \equiv m \left(\frac{2\lambda}{n} \right)^{m-1} \tag{2.21}$$

for the equilibrium constant of the chains, where $\lambda(T) \equiv [\sigma_C(\zeta-1)^2/\zeta]e^{-\beta\Delta f_0}$ is the association constant. we thus have

$$\frac{2\lambda}{n}\phi_m^C = mx^m \tag{2.22}$$

for the volume fraction of chains, where $x \equiv 2\lambda\phi_1^C/n$ is the number density of associating groups on the unassociated chains. On the contrary, equilibrium constant for the rings includes an extra factor of the probability to form a ring. This factor is proportional to $(mn)^{-3/2}$ for a Gaussian chain of length mn, but again we have to divide it by the symmetry factor $\sigma_R = m$ for a ring, because we can close a chain at any one of m bonds to form a ring. We thus have

$$K_m^R = 2^{m-1} \cdot m \left[\frac{\sigma_C(\zeta-1)^2}{n\zeta} \right]^{m-1} (e^{-\beta\Delta f_0})^{m-1} \cdot \frac{B_0}{m^{5/2}} = m \left(\frac{2\lambda}{n} \right)^{m-1} \frac{B}{m^{5/2}} \tag{2.23}$$

for rings, where $B \equiv B_0 e^{-\beta\Delta f_0}$ is a temperature dependent constant. The volume fraction of rings is given by

$$\frac{2\lambda}{n}\phi_m^R = m \cdot \frac{B}{m^{5/2}} x^m. \tag{2.24}$$

The total volume fraction of polymers is given by the sum of the two:

$$\frac{2\lambda}{n}\phi \quad = \quad \frac{2\lambda}{n}(\phi^C + \phi^R) = \sum_{m\geq 1} mx^m + B \sum_{m\geq 1} \frac{x^m}{m^{3/2}}$$

$$= \frac{x}{(1-x)^2} + B\Phi(x:3/2), \tag{2.25}$$

where the new function Φ is defined by the infinite sum

$$\Phi(x:\alpha) \equiv \sum_{m\geq 1} \frac{x^m}{m^\alpha}. \tag{2.26}$$

The upper limit of the summation is given by the maximum possible aggregation number and should not exceed the total number N of polymers, but here we have taken thermodynamic limit and let N go to infinity. The total number of clusters and molecules is similarly given by

$$\begin{aligned} \lambda\nu^S &= \lambda(1-\phi) + \sum_{m\geq 1} x^m + B\sum_{m\geq 1} \frac{x^m}{m^{5/2}} \\ &= \lambda(1-\phi) + \frac{x}{1-x} + B\Phi(x:5/2). \end{aligned} \tag{2.27}$$

Solving eq.(2.25) with respect to x and substituting the result into (2.27), we complete our general procudure, and can find equilibrium solution properties. The functions $\Phi(x:\alpha)$ with $\alpha = 3/2, 5/2$ appear in the study of Bose-Einstein condensation of ideal quantum particles [31] that obey Bose-Einstein statistics. Their mathematical properties were studied by Truesdell [32] in detail, so that it is called *Truesdell function.* Their radius of convergence is given by $x = 1$. Both function $\Phi(x:3/2)$ and $\Phi(x:5/2)$ remain at a finite value at $x = 1$, but diverge as soon as x exceeds unity. Jacobson and Stockmayer [30] showed the fraction of chains and rings on the temperature-concentration phase plane, and found very interesting phenomena that are analogous to Bose-Einstein condensation, i.e., when the parameter B exceeds a certain critical value, 100% rings are formed below a critical concentration of polymers. Such a transition originates in the singularity in Truesdell functions, and hence loop entropy, and serves as an interesting example of Bose-Einstein condensation in classical statistical mechanics.

Another singular property of this model is the divergence of the weight-average molecular weight at the point $x = 1$. The condition gives *thermal polymerization* line when mapped onto the temperature-concentration plane because at this point the average chain length goes to infity. Application of our theory gives essentially the same results as those originally found by Scott et al. [33], and later refined by Wheeler et al. [34, 35, 36]. More recently, Dudowicz et al. [37] theoretically studied living polymerization as well as thermal polymerization of sulfur along with similar consideration.

In a quite similar way, we can study mixed linear association of $R\{A_2\}$ molecules and $R\{B_2\}$ ones. The sequence distribution along an associated chain can be either alternative, sequential, or statistically random, depending upon the strength of association constants. All these associated chains, or rings, are block copolymers if the primary molecules are polymers, so that they undergo microphase separation transition as well as macroscopic phase separation. Such a problem of competing micro- and macrophase separation in associating polymers is one of the unsolved important problem to be studied.

In the case of linear association of low molecular-weight rigid molecules, the problem we are studying is related to those of fibrillar association of bifunctional molecules by (multiple) hydrogen bonds such as seen in hydrogen-bonded supramolecular liquid crystals [27, 28, 29] and low molecular weight gelators [38]. Readers can study their equilibrium properties and phase diagrams within the theoretical framework presented here. Orientational ordering of the associated mesogens in hydrogen-bonded liquid crystals will be considered in the following sections.

2.3 Side-Chain Association

Next system we study is a mixture of high molecular weight polymers $R\{A_f\}$ (DP$\equiv n_A$) bearing the number f of associative A groups and low molecular weight monofunctional molecules $R\{B_1\}$ (DP$\equiv n_B$) [39, 40], or solvent molecules S (DP$\equiv$ 1) [41]. We assume that B group, or solvent molecule, can attach onto an A group from the side of the polymer chains. Adsorption of surfactant molecules onto polymer backbones by hydrogen bonds (Figure 1.4) is an important example of the former, and hydration of water molecules in an aqueous polymer solution (Figure 1.5) is an important example of the latter. To simplify theoretical description, we write DP of molecules as $n_A \equiv na$ and $n_B \equiv nb$ by using $n \equiv n_A + n_B$. The type of clusters formed is specified by $(1, m)$ with $m = 0, 1, 2, \cdots$, while the unassociated $R\{B_1\}$ molecule is indicated by $(0, 1)$. As in the general scheme, we start with the free energy of the mixture

$$\beta\Delta F = \sum_{m=1}^{f} \Delta_m N_{1m} + N_{01} \ln \phi_{01} + \sum_{m=0}^{f} N_{1m} \ln \phi_{1m} + \Omega\chi\phi(1-\phi). \quad (2.28)$$

The volume fraction of $R\{A_f\}$ molecules is given by

$$\phi \equiv \sum_{m=0}^{f} \frac{a}{a+mb} \phi_{1m}. \quad (2.29)$$

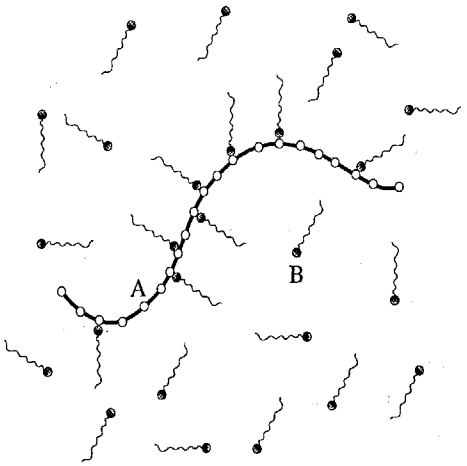

Figure 1.4. Association of end-functional low molecular-weight molecules R{B_1} from the side of a long polymer chain R{A_f}. Comb like block copolymers are formed.

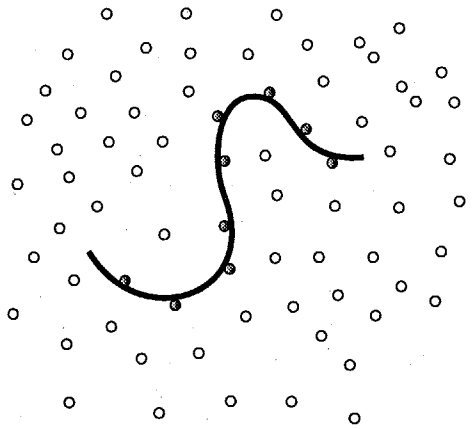

Figure 1.5. Hydration of water-soluble polymers. Water molecules S are hydrogen bonded onto a polymer chain R{A_f}, so that they partially wear cloths which are essentially the same as the surrounding solvent molecules.

The free energy required to form a $(1, m)$-mer from the primary molecules in the reference state is given by

$$\Delta_m \equiv \beta(\mu^\circ_{1m} - \mu^\circ_{10} - m\mu^\circ_{01}). \tag{2.30}$$

Chemical equilibrium conditions

$$\Delta\mu_{1m} = \Delta\mu_{10} + m\Delta\mu_{01} \tag{2.31}$$

then lead to the distribution function of the clusters

$$\phi_{1m} = K_m \phi_{10} {\phi_{01}}^m, \tag{2.32}$$

where $K_m \equiv \exp(m - \Delta_m)$ is the equilibrium constant. As usual, we split the free energy Δ_m into combinatorial, conformational and bonding terms as

$$\Delta_m = -\frac{1}{k_B}(\Delta S_{\text{comb}} + \Delta S_{\text{conf}}) + m\beta\Delta f_0. \tag{2.33}$$

The combinatorial entropy is given in terms of the number ${}_fC_m$ of different ways to attach m molecules onto f available sites on a polymer as

$$\Delta S_{\text{comb}} = k_B \ln({}_fC_m), \tag{2.34}$$

if attaching process occurs *independently*. When there is strong attractive interaction between the attached R{B_1} molecules located next to

each other along the chain, they are adsorbed in sequences, i.e., sequences with varied length of $R\{B_1\}$ molecules distribute along the polymer chain. These sequences may induce *helical order* on the main chain due to the steric hindrance of neighboring adsorbed molecules. The combinatorial factor changes to the number of different ways to select the specified sequences from the finite total length n. Such a *correlated adsorption* is recently studied in detail in relation to helix formation on polymers by adsorption of chiral molecules [40].

The conformational entropy is given by

$$\begin{aligned} \Delta S_{\rm conf}(m) &= S_{\rm dis}(n_A + mn_B) - S_{\rm dis}(n_A) - mS_{\rm dis}(n_B) \\ &= k_B \ln \left[\frac{a+bm}{a} \left\{ \frac{\sigma(\zeta-1)^2}{n_B \zeta e} \right\}^m \right] \end{aligned} \tag{2.35}$$

by using the entropy of disorientation as before.

Putting the results together, we find

$$K_m = \frac{a+bm}{a} {}_f C_m \left[\frac{\lambda(T)}{n_B} \right]^m \tag{2.36}$$

for the equilibrium constant, where $\lambda(T) \equiv [\sigma(\zeta-1)^2/e\zeta]\exp(-\beta\Delta f_0)$ is the association constant. The cluster distribution function takes the form

$$f\lambda\nu_{1m} = {}_f C_m x y^m, \tag{2.37}$$

where two unknown variables are defined by

$$x \equiv f\lambda(T)\phi_{10}/n_A \qquad \text{and} \qquad y \equiv \lambda(T)\phi_{01}/n_B. \tag{2.38}$$

These give the number density of A groups and of B groups on the molecules that remain unassociated in the solution. They are always accompanied by the association constant λ, so that the concentration can be scaled by this factor. The association constant therefore works as a *temperature shift factor* of the concentration. By counting the number of molecules and clusters moving together, we find the total number density is

$$\lambda\nu^S(x,y) = y + \frac{x}{f}(1+y)^f. \tag{2.39}$$

The coupled equations (1.20) turn into

$$x(1+y)^f = f\lambda\phi/n_A \tag{2.40a}$$

$$y + xy(1+y)^{f-1} = \lambda(1-\phi)/n_B. \tag{2.40b}$$

Since the concentrations appear together with the association constant as in the r.h.s. of these equations, we introduce new variables $c_A \equiv$

$\lambda f\phi/n_A$ and $c_B \equiv \lambda(1-\phi)/n_B$ to describe concentrations. These variables give the total number density of A groups and B groups. Solving these equations with respect to x and y, we find

$$x(\phi) = c_A/(1+y(\phi))^f \tag{2.41a}$$

$$y(\phi) = \left[c_B - c_A - 1 + \sqrt{D(\phi)}\right]/2. \tag{2.41b}$$

Substituting these results into physical properties, in particular into $\nu^S(x,y)$, we find them as functions of the temperature and concentration. For instance, the average number $< m >$ of B groups that attach to a polymer chain is given by

$$< m > \equiv \sum_{m=0}^{f} m\nu_{1m} = xy(1+y)^{f-1}/\lambda. \tag{2.42}$$

The spinodal condition becomes

$$\frac{\kappa_A(\phi)}{na\phi} + \frac{\kappa_B(\phi)}{nb(1-\phi)} - 2\chi = 0, \tag{2.43}$$

where

$$\kappa_A(\phi) = 1 - f\phi y'(\phi)/(1+y(\phi)), \tag{2.44a}$$

$$\kappa_B(\phi) = (1-\phi)y'(\phi)/y(\phi) \tag{2.44b}$$

are now functions of ϕ through c_A and c_B.

We first show theoretical phase diagrams of hydrogen-bonded comb copolymers. Ruokolainen and his coworkers [42, 43, 44, 45, 46] have recently observed MST in the mixture of poly(4-vinyl pyridine) (P4VP) and surfactant molecules 3-pentadecyl phenol (PDP). In this sytem the hydrogen bonds between the hydroxyl group in PDP and the basic aminic nitrogen in the pyridine group leads to the formation of comb-shaped block copolymers with densely grafted short side chains (called *molecular bottlebrush* [45]). They observed lamellar structures at low temperature. The lamellar period L was found to decrease in proportion to the reciprocal of x, the fraction of surfactant molecules per pyridine group in P4VP, and the MST temperature takes a minimum value (easiest MST) near the stoichiometric concentration $x = 1$. Our theory can readily be applied to study such side-chain associations [39]. An example of the phase diagram for associating comb polymers is shown in Figure 1.6. The structures of possible mesophases inside MS region were recently studied by Angerman et al. [47] by constructing RPA free energy of non-uniform systems.

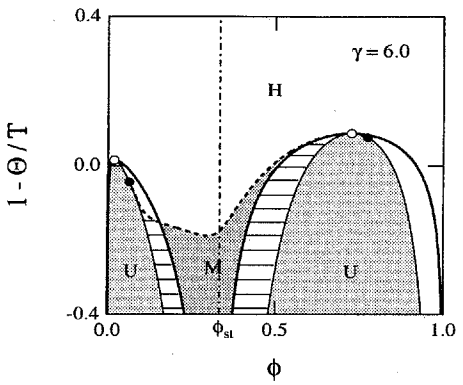

Figure 1.6. Phase diagram in which macro- and microphase separation compete by comb-shaped low-mass side-chain association. $n_A = 1000, f = 200, n_B = 10, \lambda_0 = 1.0, \gamma = 6.0$. Homogeneous liquid phase (H), microphase separated region (M), unstable region (U) are shown. MST is easiest at the stoichiometric composition indicated by ϕ_{st}. Critical solution point (white circle) and Lifshitz point (black circle) are indicated. Metastable regions inside M region are indicated by horizental thin lines. (Reprinted with permission from Ref.[39]. Copyright 1997, ACS.)

Helix induction on a polymer chain by association of hydrogen-bonding chiral molecules provides another important application of our theory. Chiral centers attached on the chain side often induce helical structures along the polymer chain by the nature of hydrogen bonds to grow in sequence. Small difference in physical interaction is non-linearly amplified by the cooperative nature of the bonds such that formation of a new bond become easier in the nearest-neighboring position to the already formed bond. Cooperative helix induction and chiral ordering in polymers with hydrogen-bonding side groups was reported by Yashima et al. [48]. In a series of experiments [48, 49, 50, 51], poly((4-carboxyphenyl)acetylene) revealed that, under the presence of chiral and achiral amines and amino alcohols in a solvent of dimethyl sulfoxide (DMSO), the optical activity measured by circular dichroism (CD) responds sharply to a slight excess of R over S form of chiral molecules (*majority effect*). It was also found that the optical activity sharply responds to small concentrations of chiral groups when achiral molecules are added. Chiral groups are therefore called "sergeants" and achiral groups "soldiers" (*sergents-and-soldiers effect*). We attempted [40] to theoretically describe such cooperative chiral ordering in polymers carrying hydrogen-bonded pendant groups within the present theoretical framework. We derived the above two major effects by directly analyzing the sequence selection process when the chiral molecules are attached onto the polymer backbone.

2.4 Hydration in Aqueous Polymer Solutions and Closed-Loop Miscibility Gap

We next present phase diagrams of aqueous polymer solutions in which water molecules are hydrogen-bonded onto polymer chains [41]. We regard the solvent molecule as $R\{B_1\}$, and fix $n_B = 1$. The DP of polymers is given by $n_A = n$. Figure 1.7 shows a possible phase diagram. In this figure, we fix the parameters as $\lambda_0 = 0.002$, and $\gamma = 3.5$ (from the measured strength of the hydrogen bond in a solution) for a typical example. The number of the statistical units on a polymer chain is varied from curve to curve. The number f of attaching sites on a polymer chain is assumed to be equal to n because each monomer carries one hydrogen-bonding oxygen. The open circles show critical solution points. The solid curves show binodals, and the dashed curves spinodals. For such a small value of λ_0, there are two miscibility gaps for low molecular-weight polymers: one ordinary miscibility dome and one closed loop above the dome (see $n = 10^2$ curve). The closed loop [9, 52, 53, 54, 55]

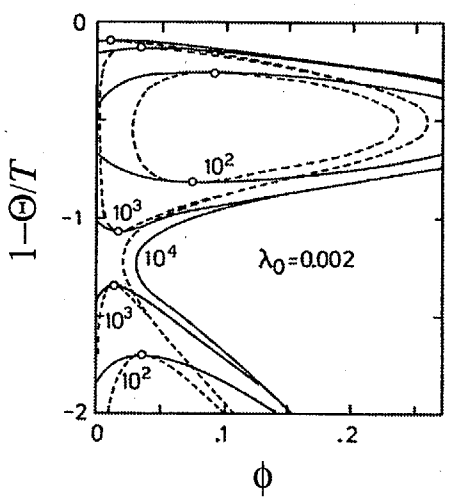

Figure 1.7. Phase diagram of hydrated polymer solutions. The segment number n is varied from curve to curve. Binodals (solid lines) and spinodals (broken lines) are drawn. The critical solution points are indicated by white circles. LCST and UCST approach and eventually merge into an hour-glass by increasing the polymer molecular weight. The phase separation loop vanishes by decreasing the polymer molecular weight. (Reprinted with permission from Ref.[41]. Copyright 1990, APS.)

has one *upper critical solution temperature* (UCST) on the top and one *lower critical solution temperature* (LCST) at the bottom. The dome has an ordinary UCST. As the molecular weight is increased, the LCST

and the UCST of the dome come closer and closer, and at a certain value of n (1670 for the parameters given in this figure) the two points merge into a higher order critical point (called *double critical point* [56]). For a molecular weight higher than this critical value, the two gaps merge into a single *hourglass* shape. On the contrary, the miscibility loop shrinks with decrease in the molecular weight, and eventually vanishes at a certain critical molecular weight ($n = 37$ for the Figure 1.7). This vanishing loop is called *hypercritical point.* For a slightly higher value of λ_0, however, it was found that the two gaps remain separated no matter how large the molecular weight may become [41]. There are three theta temperatures under such condition to which each critical point approaches in the limit of infinite molecular weight. For a still larger value of λ_0, the closed loop does not appear, and we are left with an ordinary miscibility dome only. Since the parameter λ_0 is small if the entropy loss during the bond formation is large, there must be a strong orientational or configurational constraint in the local geometry for the appearance of an hourglass.

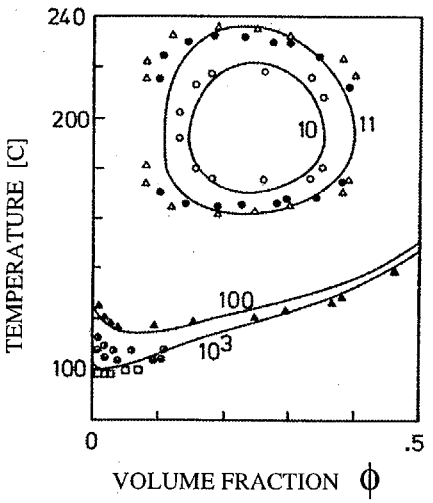

Figure 1.8. Phase diagram of aqueous poly(ethylene oxide) (PEO) showing closed-loop miscibility gap. Theoretical curves are fitted to the experimental data of the cloud points measured by Saeki et al. The miscibility loop expands with increase in the molecular weight. The UCST phase separation expected at low temperature cannot be observed due to crystalization of PEO. (Reprinted with permission from Ref.[41]. Copyright 1990, APS.)

Figure 1.8 shows a comparison [41] of the theoretical calculation with the observed phase diagram [57, 58] of polyethylene oxide (PEO) in water. The number-average molecular weight in the experiment covers the range $2.17 \times 10^3 - 1.02 \times 10^6$. The solid curves show the calculated binodals. The number n of the statistical units on a chain is varied from curve to curve. Parameters used for fitting are: $\psi_1 = 1, \Theta = 730$ K, $\gamma = 6$, and $\lambda_0 = 1.66 \times 10^{-5}$. Fitting is made mainly by adjusting the unkown parameter λ_0. The agreement is very good. Calculation of PEO/water phase diagrams was later examined by taking the hydrogen-bond networks in water into account [59]. Effect of pressure on the miscibility loop was studied to derive temperature-pressure phase diagrams [60].

2.5 Hydrogen-Bonded Liquid-Crystalline Supramolecules

Some rigid molecules are known to undergo liquid crystallization when hydrogen-bonded to each other. For a binary mixture of low-mass molecules, as well as polymers, R{A} and R{B}, each carrying at least one rigid part A and B that form mesogenic core when associated, dimer type, trimer type, main-chain type, side-chain type, combined type, and network type are known [29, 61]. These are called *hydrogen-bonded supramolecular liquid crystals*. For example, aromatic acid derivatives with alkoxy or alkyl terminal groups form dimers due to hydrogen bond between their carboxylic acid groups, and show mesomorphism [62, 63, 64, 65]. Association between different species of molecules also induces the isotropic/anisotropic phase transition [29, 66, 67]. Most remarkable one is the case that non-mesogenic molecules form compounds with mesogenic cores when hydrogen-bonded. In such combinations of molecules, isotropic materials undergo liquid crystallization by simple mixing.

To describe liquid crystallization by association, we introduce orientational free energy in addition to the free energy of reaction and mixing. Let us assume that R{A_f} molecule carries the number f of linear rigid associative groups A of length n_A^* , and R{B_g} molecule does the number g of rigid groups B of length n_B^*. The total DPs are $n_A = n_A' + f n_A^*$ and $n_B = n_B' + g n_B^*$. For the orientational free energy, we employ conventional molecular field theory of Maier and Saupe [68], or its extension by McMillan [69] that includes both orientational ordering of the mesogenic cores and translational ordering of their center of mass. It is given by

$$\beta \Delta F_{\text{ori}} = \left\{ (-\ln Z) + \frac{1}{2} \zeta (\eta^2 + \alpha \sigma^2) \nu_M \right\} N_M, \qquad (2.45)$$

where N_M is the total number of mesogenic cores formed in the system, and $\nu_M \equiv N_M/\Omega$ is their number density. In contrast to the conventional liquid crystals, they are variables that change depending on the temperature and composition, and should be decided by the equilibrium condition. The symbol η expresses nematic order parameter defined by

$$\eta \equiv < P_2(\cos\theta) >, \tag{2.46}$$

and similarly

$$\sigma \equiv < P_2(\cos\theta)\cos(2\pi z/d) > \tag{2.47}$$

is the smectic order parameter. (The function $P_2(x) \equiv (3x^2-1)/2$ is the Legendre polynomial of degree 2.) The coupling constant ζ (Maier-Saupe's interaction parameter) shows nematic interaction parameter, and α shows McMillan's smectic interaction parameter. The averages refer to the statistical weight for orientation of each mesogenic core, whose partition function Z is defined by

$$Z(\eta,\sigma) \equiv \frac{1}{d}\int_0^d dz \int_0^1 d\cos\theta \exp\left\{\zeta\left[\eta + \alpha\sigma\cos(2\pi z/d)\right] P_2(\cos\theta)\nu_M\right\}, \tag{2.48}$$

where d is the distance between the neighboring planes in a smectic A structure on which the centers of mass of mesogenic cores are located (layer thickness). The symbol θ shows the angle of the longitudinal axis of each mesogenic core measured from the preferential orientational axis. By using this statistical weight, the definitions (2.46) and (2.47) become self-consistent coupled equations to find the order parmeters. We first solve these equations with equilibrium conditions for ν_M, and then by substitution find the chemical potential of each component as functions of the temperature and composition. We show an example of the phase diagram calculted by this theoretical framework in the case of dimer formation [70]. Figure 1.9 shows a phase diagram of a symmetric mixture with $n_A = n_B = 10$, and $n_A^* = n_B^* = 1$ (small rigid head groups carrying short alyphatic flexible tails). Temperature is measured by $t \equiv T/T_{NI}$ in the unit of the nematic/isotropic transition temperature T_{NI}. We have assumed that Flory's χ-parameter takes the form $\chi \equiv C_1 + C_2/t$ using the reduced temperature t with C_1 and C_2 constants specified by the combination of molecular species. They are fixed at $C_1 = -0.5$ and $C_2 = 0.05$. The association constant is assumed to take the form $\lambda(T) = \lambda_0 \exp(C/t)$, where $C \equiv |\Delta\epsilon|/k_B T_{NI}$ is the dimensionless energy of the hydrogen bond. We have fixed at $\lambda_0 = 30.0$ and $C = 0.3$. The inset magnifies the important part in the Figure. Thin solid line is the I/N transition line, and thick solid line the N/S_m transition line. Letters I, N, and S_m represent the state whose free energy is lowest

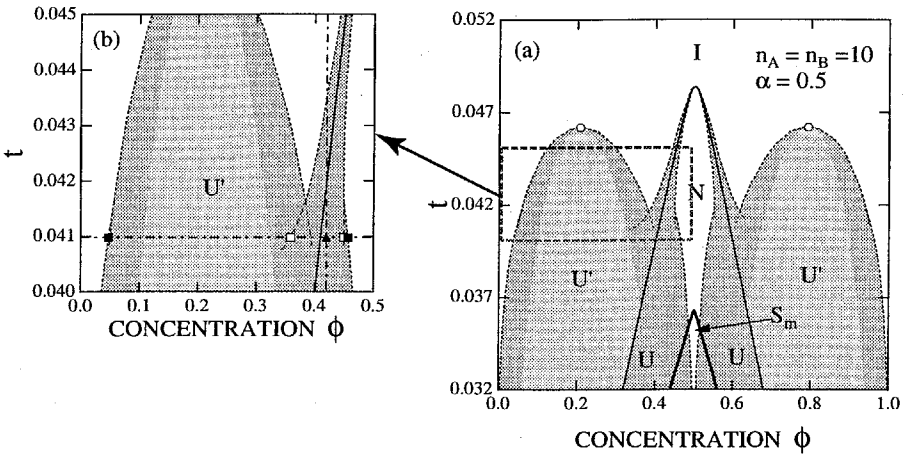

Figure 1.9. Phase diagram of dimer-forming hydrogen-bonded supramolecular liquid crystal, and its partial magnification. Thin solid line is the I/N transition line, thick solid line is the N/S_m transition line, and dotted line is the binodal. The hatched area is the metastable region. The dark gray area with "U" is the unstable region due to entropy difference between two different species of N structures. The light gray area with "U′" is the unstable region due to mixing two different species of molecules. White circle represents the critical solution point. Parameters are fixed at $n_A = n_B = 10$, $n_A^* = n_B^* = 1$, $\lambda_0 = 30.0$, $C = 0.3$, $C_1 = -0.5$, $C_2 = 0.05$, and $\alpha = 0.5$. (Reprinted with permission from Ref.[70]. Copyright 2002, ACS.)

in the area. Dotted lines limiting the hatched metastable region are binodals. The dark gray area indicated by U is the unstable region that is hidden inside the coexistent region, whereas the light gray area with U′ is the conventional unstable region due to demixing. White circles represent critical solution points. An unstable region hidden in a two-phase coexistence region due to the first order nature is well known in metallurgy as metastable phase boundary [71]. Recently the existence of the spinodal curve hidden in a metastable region has been a focus of study on crystallization of polymers [72, 73]. These hidden unstable regions usually accompany the first order phase transitions, and lie in the region where the liquid state has the lowest free energy.

At high temperature, the coexistence region caused by first order I/N phase transition, and also that caused by demixing the two different species of molecules appear. Depending upon the composition, the mixture separates either into two I phases by the effect of mixing enthalpy or into I phase and N phase by the I/N transition. At intermediate temperature, the two coexistence regions merge, but the U region and the U′

region remain separated. From such a structure of the phase diagram, two-step spinodal decomposition is possible; the mixture first separates into two metastable I phases or metastable I and N phase, and then into stable I and N phase. For example, when the mixture is quenched to black triangle point from a high temperature shown in Figure 1.9 (b), it separates temporarily into metastable I and N phase (white square) by the driving force based on the I/N transition, and eventually into stable I and N phase (black square) by cooperative driving force due to the I/N transition and the usual demixing. It is, however, also possible that larger fluctuations in spinodal decomposition lead to direct separation into stable I and N phase. At lower temperature, two unstable regions U and U′ also merge, so that the mixture separates directly into stable I and N phase, or into stable I and S_m phase by the cooperative driving force. If we divide the phase diagram into two at the middle and see the left half, it is similar to a theoretical phase diagram of a lyotropic liquid crystal first derived by Flory [74], and later confirmed by an experiment by Miller et al. [75]. The narrow I/N coexisting region extending from the macroscopic phase separation region is called miscibility *chimney.* In lyotropic liquid crystals, the chimney goes straight up to high temperature, but our results show that there is a limiting temperature (the top of N phase) to which the chimney approaches, because the number of mesogenic cores decreases with increasing temperature.

3. GELLING SOLUTIONS AND MIXTURES

Let us move onto gelling solutions. We first study simple pairwise association of functional groups, then generalize the theory to multiple association. Finally, we study complex mixtures where networks are formed by more than one species of polymers.

3.1 Micellization and Gelation

We start with a simple model binary mixture [12, 13, 14] in which solute molecules $R\{A_f\}$ of the molecular weight $n_A \equiv n$, each carrying f identical functional groups A, are mixed with low molecular weight ($n_B = 1$) solvent molecules S. The solute molecules can be low molecular-weight functional molecules as well as polymers carrying functional groups. Pairwise association between A groups only is assumed ($\lambda_{AA} > 0, \lambda_{AB} = \lambda_{BB} = 0$). In equilibrium state we have solvent $(0,1)$ and l-mers $(l,0)$, where $l = 1, 2, 3....$ To simplify the symbols, we contract the double suffices into single ones, and write l for an l-mer, 0 for

a solvent. Our starting free energy is given by

$$\beta\Delta F = \sum_{l\geq 1} N_l \ln \phi_l + N_0 \ln \phi_0 + \chi\phi(1-\phi)\Omega + \sum_{l\geq 1} \Delta_l N_l + \delta(\phi) N^G, \quad (3.1)$$

where $\phi_0 \equiv 1-\phi$ is the volume fraction of the solvent, N^G the number of $\mathrm{R}\{\mathrm{A}_f\}$ molecules in the macroscopic cluster if exists. In general, such a macroscopic cluster can take any structure as far as its molecular weight is infinite; it can be a three dimensional branched network, a worm-like micelle, an infinitely long string, etc. But, in what follows, we mainly concern networks. Let us first find a simple criterion for gelling with regard to the size of of the aggregate clusters.

By differentiation, we find for chemical potentials

$$\beta\Delta\mu_l = \Delta_l + 1 + \ln\phi_l - nl\nu^S + \chi nl(1-\phi)^2 + nl\delta'(\phi)\nu^G(1-\phi), \quad (3.2a)$$

$$\beta\Delta\mu_0 = 1 + \ln(1-\phi) - \nu^S + \chi\phi^2 - \delta'(\phi)\nu^G\phi. \quad (3.2b)$$

Our general procedure developed above for chemical equilibrium leads to the volume fraction of the clusters to be given by

$$\phi_l = K_l {\phi_1}^l, \quad (3.3)$$

where ϕ_1 is the volume fraction of the unassociated molecules, and the equilibrium constant is given by

$$K_l = \exp(l - 1 - \Delta_l). \quad (3.4)$$

We then consider the total amount of materials in the sol:

$$\phi^S(x,y) = y + \sum_{l=1}^{\infty} K_l x^l, \quad (3.5)$$

where $x \equiv \phi_1$ for the solute molecules and $y \equiv 1-\phi$ for the solvent. To study convergence of the infinite summation in this equation, let us define the free energy gain $\delta_l \equiv \Delta_l/l$ produced when a single chain participates in a cluster of the size l. Application of the Cauchy-Hadamard's theorem [76] gives the convergence radius x^* of the power series in the form

$$1/x^* = \overline{\lim_{l\to\infty}}(K_l)^{1/l} = e^{1-\delta_\infty}, \quad (3.6)$$

where the least upper bound of the limit has been indicated by a bar. The quatity $\delta_\infty \equiv \lim_{l\to\infty}\delta_l$ is defined by the limiting value of δ_l as $l \to \infty$. In the present special case of self assembly, we have a linear boundary in the unit square on the (x,y) plane which is parallel to the

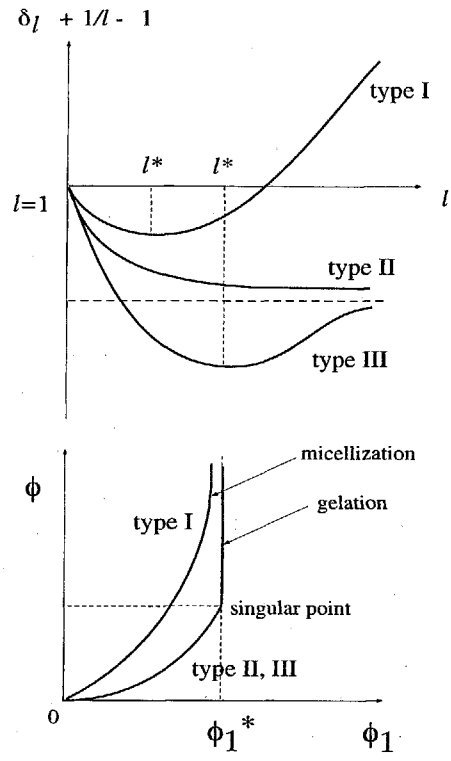

Figure 1.10. (Top) The binding free energy per molecule as functions of the aggregation number. (Bottom) Total volume fraction as a function of the unimer concentration. Type I leads to micellization with finite aggregation number. Type II and Type III lead to macroscopic aggregates, such as infinitely long cylindrical micelles, three dimensional networks. In the latter case, the volume fraction ϕ_1 of the molecules that remain unassociated in the solution as a function of the total volume fraction ϕ of the molecules shows a singularity at the point where the weight average molecular weight of aggregates becomes infinite.

y-axis. Within the radius of convergence, the normalization condition $\phi^S(x, y) = 1$ gives one-to-one relationship between ϕ and x. Formation of several different spatial structures can be seen from the behavior of δ_l. Figure 1.10 schematically shows the exponent $\delta_l + 1/l - 1$ in the equilibrium constant $K_l^{-1/l}$ as a function of l. This function may either take a minimum at a certain finite l (curve (I) and (III) of Figure 1.10) or decreases monotonically to a finite value $\delta_\infty - 1$ (curve (II)). Let l_0 be the value of l at which the curve reaches the minimum (including $l_0 = \infty$ for the monotonic case). The cluster size l for which the volume

fraction ϕ_l becomes largest is given by

$$\partial\Delta_l/\partial l = 1 + \ln x. \tag{3.7}$$

Let l^* be the solution of this equation for the value of x at the convergence radius x^*. In the case where l^* is finite, the total concentration corresponding to the upper bound x^* is called *critical micelle concentration* (cmc), since the volume fraction of the clusters with aggregation number l^* goes up to a finite fraction at this value of the total volume fraction [77]. Sharpness in their appearance is controlled by the curvature of the function $\delta_l + 1/l - 1$ around l^*. At cmc, we have $l_0 = l^*$.

In the case where l^* is infinite, on the contrary, a macroscopic cluster appears as soon as x exceeds the critical value $x^* \equiv \exp(\delta^* - 1)$. The macroscopic clusters can be branched networks (gels) [4, 5], infinitely long polymers [33], or wormlike micelles [78, 79, 80]. For brevity, we call the former case *gelation* and the latter case *polymerization* (including worm-like micellization. (Precisely, worm-like micelles formed by hydrophobic association fall on the category of multiple association described below. Here, we roughly call one-dimensional self assembled object worm-like micelle.) The total concentration ϕ^* obtained from x^* gives the concentration at which this transition takes place. It depends on temperature through δ_∞. For ϕ above ϕ^*, the sum in $\phi^S(x, y)$ cannot reach ϕ. The amount of shortage $\phi - \sum \phi_l$ condensates into the macroscopic clusters.

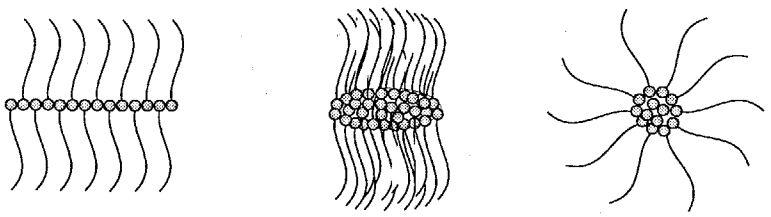

Figure 1.11. Micellization of end-associative polymer chains. (a) linear association (b) two-dimensional discotic association (c) three-dimensional spherical association

Let us see simple examples. When molecules form linear array as in Figure 1.11 (a), the internal free energy of an aggregate is $\mu_l^\circ = -(l-1)\alpha k_B T$, where $\alpha k_B T$ is the free energy of a bond. We have

$$\delta_l + 1/l - 1 = -(1-\alpha) + \alpha/l^p + 1/l \tag{3.8}$$

with $p = 1$. For two dimensional disk-like aggregates as in Figure 1.11 (b), we have the same equation with $p = 1/2$, because the aggregation

number l is proportional to the area πR^2, and there are no bonds from outside along the edge. Similarly, we have $p = 1/3$ for three dimensional aggregates as in Figure 1.11 (c). All these examples give monotonically decreasing curve of type II, and hence $(\phi_1)_{\rm cmc} = \exp[-(1+\alpha)]$ for the critical micelle concentration. Above the cmc, the unimer concentration is nearly fixed at this value, and the volume fraction of aggregates with specified number is given by $\phi_l \simeq \exp\left[-(1+\alpha l^{1-p})\right]$, or

$$\phi_l \simeq \begin{cases} e^{-\alpha} & (p=1) \\ e^{-\alpha l^{1/2}} & \ll 1 \quad (p=1/2) \\ e^{-\alpha l^{2/3}} & \ll 1 \quad (p=1/3) \end{cases} \tag{3.9}$$

We therefore expect widely polydisperse distribution for linear aggregates because ϕ_l is almost constant. For two and three dimensional aggregates, distribution function decays quickly with the aggregation number, and, since the total concentration is a given variable, aggregates of infinite size easily appear.

Let us next consider the type I and type III where stable micelles of finite size are formed. We expand the binding free energy around l^* as

$$1 - \delta_l - \frac{1}{l} \cong a - b(l-l^*)^2 + \cdots, \tag{3.10}$$

where a, b are positive constants. Since the volume fraction of l-mers is given by

$$\phi_l = e^{-bl(\Delta l)^2}(e^a \phi_1)^l, \tag{3.11}$$

cmc is decided from the condition

$$(\phi_1)_{\rm cmc} = e^{-a}. \tag{3.12}$$

Hence we have

$$\phi_l \cong e^{-l^* b(\Delta l)^2} \tag{3.13}$$

near around $l = l^*$, i.e., the distribution function of micelles becomes Gaussian with mean value l^* and variance $1/\sqrt{2l^*b}$.

3.2 Gelation by Pairwise Association

Let us consider the simplest gelling binary mixture in which primary functional molecules form networks in a solvent [10, 11, 12]. In order to derive the equilibrium constants in an analytical form, let us introduce a simple model for the internal structure of clusters. Clusters are assumed to take tree structure with no internal loops (called *Cayley tree*). Cycle formation within a cluster is neglected. This is a crude approximation

on the basis of the classical theory of gelation [8, 81, 82], but in fact it is known to work very well before the gel point is reached.

Our general theoretical scheme gives for the chemical potentials of the clusters and solvent as

$$\beta\Delta\mu_l = \Delta_l + 1 + \ln\phi_l - nl\nu^S + \chi nl(1-\phi)^2 + nl\delta'(\phi)\nu^G(1-\phi) \tag{3.14a}$$

$$\beta\Delta\mu_0 = 1 + \ln(1-\phi) - \nu^S + \chi\phi^2 - \delta'(\phi)\nu^G\phi, \tag{3.14b}$$

where

$$\nu^S \equiv \sum \nu_l + 1 - \phi \tag{3.15}$$

gives the total number of molecules and clusters having translational degree of freedom. As usual, we now split the free energy into three parts:

$$\Delta_l = \Delta_l^{\text{comb}} + \Delta_l^{\text{conf}} + \Delta_l^{\text{bond}}. \tag{3.16}$$

To find the combinatorial part, we employ the entropy change on combining l identical f-functional molecules to form a single Cayley tree. The classical tree statistics [82] gives

$$\Delta S_l^{\text{comb}} = k_B \ln[f^l\omega_l], \tag{3.17}$$

where

$$\omega_l \equiv \frac{(fl-l)!}{l!(fl-2l+2)!} \tag{3.18}$$

is Stockmayer's combinatorial factor [82]. The free energy is given by $\Delta_l^{\text{comb}} = -\Delta S_l^{\text{comb}}/k_B$.

For the conformational free energy, we again employ the lattice theoretical entropy of disorientation (2.12), and find

$$\Delta S_l^{\text{conf}} = S_{\text{dis}}(ln) - lS_{\text{dis}}(n) = k_B \ln\left[\left(\frac{\sigma(\zeta-1)^2}{\zeta en}\right)^{l-1} l\right]. \tag{3.19}$$

Finally, free energy of bonding is given by

$$\Delta_l^{\text{bond}} = (l-1)\beta\Delta f_0 \tag{3.20}$$

because there are $l-1$ bonds in a tree of l molecules, where Δf_0 is the free energy change on forming a single bond.

Combining all results together, we find

$$K_l = fl\omega_l\left(\frac{f\lambda}{n}\right)^{l-1} \tag{3.21}$$

for the equilibrium constant, where

$$\lambda(T) \equiv [\sigma(\zeta-1)^2/\zeta e]\exp(-\beta\Delta f_0) \tag{3.22}$$

is the association constant. The distribution of clusters (3.3) then gives

$$\lambda\nu_l = \omega_l x^l \tag{3.23}$$

for the number density, where the independent variable x here is defined by

$$x \equiv f\lambda\phi_1/n = f\lambda\nu_1, \tag{3.24}$$

which gives the number of functional groups $f\phi_1/n$ carried by the unassociated polymer chains in the solution multiplied by the association constant $\lambda(T)$ as a temperature shift factor. From this distribution function, we can obtain average values of physical quantities. First, the total number concentration of the finite clusters is given by

$$\lambda\sum_{l\geq 1}\nu_l = S_0(x). \tag{3.25}$$

Their volume fraction is

$$\frac{\lambda}{n}\sum_{l\geq 1}\phi_l = S_1(x) \tag{3.26}$$

Therefore, the number average of the cluster size is given by

$$\bar{l}_{\rm n} \equiv \sum l\nu_l / \sum \nu_l = S_1(x)/S_0(x) \tag{3.27}$$

and the weight average is

$$\bar{l}_{\rm w} \equiv \sum l^2\nu_l / \sum l\nu_l = S_2(x)/S_1(x) \tag{3.28}$$

These are written in terms of the moments of Stockmayer's distribution function defined by

$$S_k(x) \equiv \sum_{l=1}^{\infty} l^k\omega_l x^l \quad (k=0,1,2\cdots). \tag{3.29}$$

These moments are explicitly written in terms of the extent α of reaction defined by the equation

$$x \equiv \alpha(1-\alpha)^{f-2}. \tag{3.30}$$

For instance,

$$S_0(x) = \alpha(1-f\alpha/2)/f(1-\alpha)^2, \tag{3.31a}$$

$$S_1(x) = \alpha/f(1-\alpha)^2, \tag{3.31b}$$

$$S_2(x) = \alpha(1+\alpha)/f[1-(f-1)\alpha](1-\alpha)^2. \tag{3.31c}$$

To see the physical meaning of α, let us calculate the probability for a randomly chosen functional group to be associated. Since an l-mer includes the total of fl groups, among which $2(l-1)$ are associated. Hence the probability of association (extent of reaction) is given by

$$2[S_1(x) - S_0(x)]/fS_1(x) = \alpha. \tag{3.32}$$

Thus, α gives the extent of association.

By using α, the average cluster sizes are given by

$$\bar{l}_{\rm n} = 1/(1 - f\alpha/2) \equiv P_{\rm n}(\alpha) \tag{3.33a}$$
$$\bar{l}_{\rm w} = (1+\alpha)/[1-(f-1)\alpha] \equiv P_{\rm w}(\alpha). \tag{3.33b}$$

3.2.1 Pregel Regime. The weight average diverges at $\alpha = 1/(f-1)$. This suggests that $\alpha = \alpha^* \equiv 1/(f-1)$ is the gel point. The number average also diverges at $\alpha = 2/f$, but since $2/f > 1/(f-1)$, we have to study the postgel regime to examine its behavior. In the pregel regime where $\alpha < \alpha^*$ holds, the volume fraction ϕ^S occupied by the polymer chains belonging to the sol must always be equal to the total polymer volume fraction ϕ since no gel network exists. Thus the total polymer volume fraction ϕ and the extent of association α satisfy the relation

$$\frac{f\lambda}{n}\phi = \frac{\alpha}{(1-\alpha)^2}. \tag{3.34}$$

We can solve this equation for α. The result can be expressed as

$$\alpha = \frac{1}{2c}\left\{1 + 2c - \sqrt{1+4c}\right\} \tag{3.35}$$

in terms of the number concentration

$$c \equiv \frac{f\lambda(T)}{n}\phi \tag{3.36}$$

of the functional groups (with the temperature shift factor of the association constant). We can then express all physical quantities directly in terms of c. For instance, the total free energy per lattice cell is given by

$$\frac{\beta\Delta F}{\Omega} = \frac{\phi}{n}\left\{(f-2)\ln(1-\alpha) + \ln\alpha + \frac{1}{2}f\alpha\right\} + (1-\phi)\ln(1-\phi) + \chi\phi(1-\phi). \tag{3.37}$$

Hence the renormalization of the χ-parameter by association turns out to be

$$\Delta\chi(\phi) = \left[(f-2)\ln(1-\alpha) + \ln\alpha + \frac{1}{2}f\alpha - \ln\phi\right]/n(1-\phi). \tag{3.38}$$

We thus find the molecular origin of the concentration dependence of χ-parameter in associating polymer solutions. In a similar way, the spinodal condition is given by

$$\frac{\kappa(\phi)}{n\phi} + \frac{1}{1-\phi} - 2\chi = 0, \tag{3.39}$$

where a new function κ is defined by

$$\kappa(\phi) = \frac{1-(f-1)\alpha}{1+\alpha} = \frac{1}{P_{\mathrm{w}}(\alpha)} \tag{3.40}$$

with α given by (3.35). It is the reciprocal of the weight-average cluster size.

3.2.2 Gel Point. Let us next find the sol/gel transition point. The free energy change δ_l per molecule is a steadily decreasing function of l, approarching the limiting value $\delta_\infty = 1-(f-1)\ln(f-1)+(f-2)\ln(f-2)-\ln\lambda(T)$. This model therefore falls on the category II in the Figure 1.10. This limit gives for the convergence radius of the series (3.29)

$$\phi_1^* = \exp(\delta_\infty - 1)$$

or, equivalently,

$$x^* = (f-2)^{f-2}/(f-1)^{f-1} \tag{3.41}$$

in terms of x, and

$$\alpha^* = 1/(f-1)$$

in terms of the extent of association as was expected from the divergence of $\bar{l}_{\mathrm{w}}$. The volume fraction of polymers at the gel point is then given by

$$\frac{\lambda(T)}{n}\phi^* = \frac{f-1}{f(f-2)^2} \tag{3.42}$$

This gives sol/gel transition line on the temperature-concentration plane.

3.2.3 Postgel Regime. In the postgel regime where $\phi > \phi^*$ and $\alpha > \alpha^*$, we have additional balance condition between the chemical potential of a polymer chain in the sol part and the one in the gel part [83]. This equilibrium condition $\Delta\mu_1 = \Delta\mu^G$ gives

$$\ln x = \delta(\phi) - 1. \tag{3.43}$$

Here, the free energy $\delta(\phi)$ produced on binding a chain onto the gel network should depend upon the concentration because the structure of

the gel changes. It starts with the initial value δ_∞ at the gel point, i.e., $\delta(\phi^*) = \delta_\infty$. Thus, the volume fraction of the unreacted chains is related to the binding free energy.

Since the conversion in the sol can in general be different from that in the gel, let us write the former as α' and the latter as α''. The average conversion α of the solution as a whole is given by

$$\alpha = \alpha' w^S + \alpha'' w^G. \tag{3.44}$$

The volume fraction ϕ^S of polymers belonging to the sol is consequently given by

$$\lambda \phi^S / n = S_1(\alpha') \tag{3.45}$$

in the postgel regime, so that it is different from the total ϕ that is given in terms of α. The sol fraction w^S is given by

$$w^S \equiv \phi^S / \phi = S_1(\alpha')/S_1(\alpha), \tag{3.46}$$

and hence the gel fraction is given by

$$w^G = 1 - S_1(\alpha')/S_1(\alpha). \tag{3.47}$$

The number ν^S of the total clusters in the chemical potentials must also be replaced by

$$\nu^S = S_0(\alpha')/\lambda + 1 - \phi \tag{3.48}$$

since it must give the number of molecules and clusters that have translational degree of freedom. The gel network spans the entire solution and loses translational motion. By using this ν^S, the chemical potentials are given by

$$\frac{\beta \Delta \mu_1^*}{n} = \frac{1 + \ln x}{n} - \nu^S + \chi(1-\phi)^2 + \delta'(\phi)(1-\phi)\nu^G, \tag{3.49a}$$

$$\beta \Delta \mu_0^* = 1 + \ln(1-\phi) - \nu^S + \chi\phi^2 - \delta'(\phi)\phi\nu^G. \tag{3.49b}$$

The function κ in the spinodal condition takes a form

$$\kappa(\phi) = \frac{d}{d\ln\phi}\left(1 + w^G \frac{d}{d\ln\phi}\right) \ln x(\alpha'), \tag{3.50}$$

which is different from the one in the pregel regime. Explicitly, it becomes

$$\kappa(\phi) = \left[1 + w^S\left(1 - \frac{P_w(\alpha')}{P_w(\alpha)}\right)\right] \frac{1}{P_w(\alpha)} + w^G \frac{d}{d\ln\phi}\left(\frac{1}{P_w(\alpha)}\right). \tag{3.51}$$

(1) Flory's treatment

By the definition (3.30) of α, x takes a maximum value $x^* = (f -$

$2)^{f-2}/(f-1)^{f-1}$ at $\alpha = 1/(f-1)$. Therefore, two values of α can be found for a given value of x. Let us consider the postgel regime $\alpha > \alpha^*$. For a given α, the value of x is fixed by the relation $x \equiv \alpha(1-\alpha)^{f-2}$. Flory postulated [8] that another root α' lying below α^* of this equation for a given value of x gives the extent of reaction in the sol. The larger one of α lying above α^* gives that for all functional groups in the system. The volume fraction ϕ^S of polymers in the sol is then given by

$$\frac{\lambda}{n}\phi^S = \frac{\alpha'}{f(1-\alpha')^2}, \tag{3.52}$$

and the gel fraction is given by

$$w^G = 1 - w^S = 1 - (1-\alpha)^2\alpha'/(1-\alpha')^2\alpha. \tag{3.53}$$

Hence, the gel fraction reaches unity only at the limit of complete reaction $\alpha = 1$. The extent of association α'' in the gel can be obtained by eq.(3.44). Explicitly, it gives

$$\alpha'' = [(1-\alpha')^2\alpha^2 - (1-\alpha)^2\alpha'^2]/[(1-\alpha')^2\alpha - (1-\alpha)^2\alpha']. \tag{3.54}$$

This value is larger than that given by the infinite limit in the tree approximation

$$\lim_{l\to\infty}[(f-2)l+2]/fl = 2/f, \tag{3.55}$$

so that, in Flory's picture, cycle formation is allowed within the gel network. The binding free energy $\delta(\phi)$ of a chain onto the gel network is then given by

$$\delta(c) = 1 - (f-1)\ln c + f\ln[(\sqrt{1+4c}-1)/2]. \tag{3.56}$$

As shown in Figure 1.12, the absolute value of the binding free energy is a monotonically increasing function of the concentration. With increase in the concentration, the network structure becomes tighter, so that binding of a polymer chain becomes stronger. The main results obtained by Flory's picture are summerized in Figure 1.13.

(2) Stockmayer's treatment

However, Stockmayer [82] later remarked that Flory's result in the postgel regime is inconsistent with the tree assumption, since the treatment permits cycle formation in the gel network. To remove this inconsistency, he proposed another treatment of the postgel regime. He introduced a different assumption that the extent of reaction of functional groups in the finite clusters remains at the critical value $1/(f-1)$ throughout the

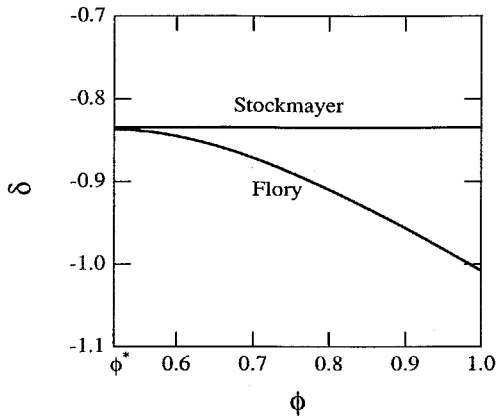

Figure 1.12. The dimensionless binding free energy in the postgel regime in two treatments. In Flory's treatment, the absolute value of the binding free energy increases with the concentration because the number of junctions on a chain increases on average.

postgel regime. He also proposed that in the postgel regime the extent of association in the gel network takes the value $\alpha'' = 2/f$ appropriate to an infinite tree structure without cycles. The weight fraction w^G of the gel then takes the form

$$w^G = \frac{(f-1)\alpha - 1}{1 - 2/f}, \tag{3.57}$$

where α ($> \alpha^*$) is the extent of reaction including all functional groups. It is a linear function of α, and reaches unity at $\alpha = 2/f$ before reaction is completed. The volume fraction of the sol ϕ^S remains constant at $\phi^S = \phi^*$. The number-average DP remains constant at $\bar{l}_n = (f-2)/2(f-1)$, while the weight-average is divergent $\bar{l}_w = \infty$ in the postgel regime. The binding free energy is fixed at δ_∞. From a physical viewpoint, Flory's model is closer to reality, since intramolecular connection is an essential feature of the network structure. The main results obtained by Stockmayer's picture are summerized in Figure 1.14.

Figure 1.15 compares phase diagrams calculated by the two different treatments of the postgel regime [83]. Binodals and spinodals appear in different positions. For the same association constant, Stockmayer's treatment gives a tricritical point (TCP) [84, 85] at the crossing of sol/gel transition line and binodal (spinodal), while Flory's treatment gives a

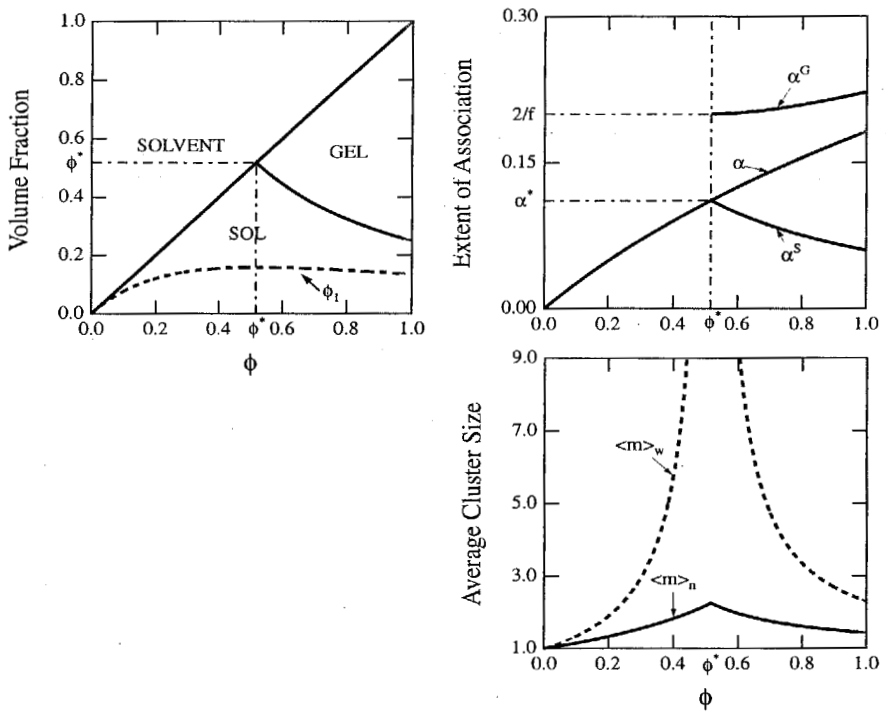

Figure 1.13. The gel fraction, the extent of association and the average molecular weight calculated on the basis of Flory's postgel picture. The number-average has discontinuous slope across the gel point, while the weight average diverges.

critical endpoint (CEP) [85] at the shoulder of the binodal and a critical point (CP) in the postgel regime. This is possible because Flory's treatment allows cycle formation within the gel network. Existence of a CP in the postgel regime suggests that phase separation between dilute gel (with only a few cycles) and concentrated gel (with many cycles) in the postgel regime is possible.

In Figure 1.16, we show a comparison between experimental phase diagram of atactic polystyrene (at-PS) solution in carbon disulfide (CS_2) [86, 87, 88] and its theoretical calculation. This solution shows TCP type phase diagram, but CEP types were also reported for at-PS in different solvents [87]. Here, we attempted to fit the data by simple pairwise crosslinking in Stockmayer's picture. The molecular origin of crosslinking has been the subject of a great deal of works [4, 87, 89, 90],

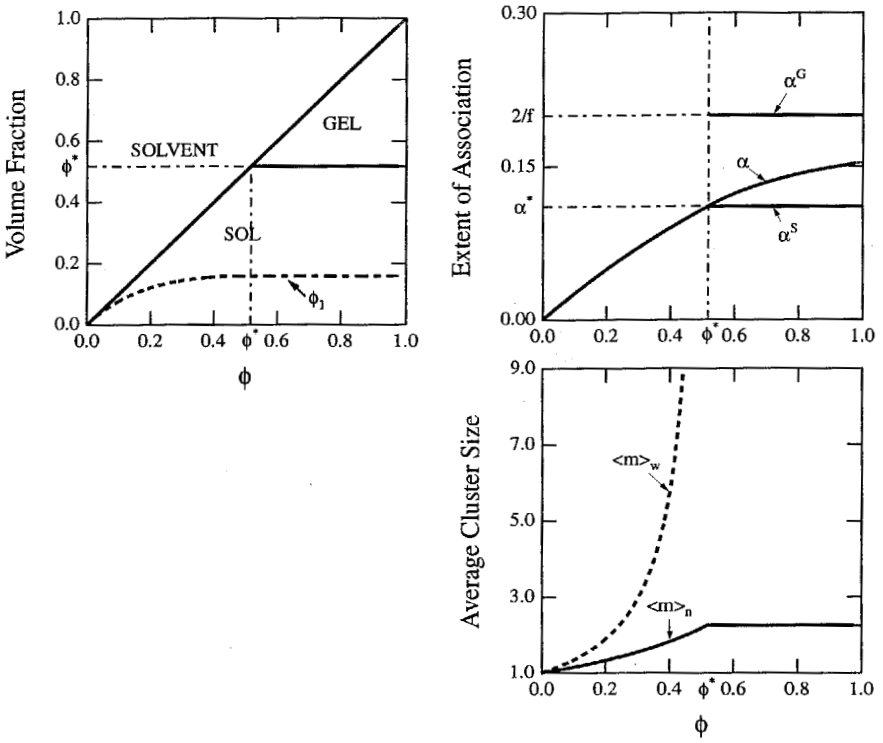

Figure 1.14. The gel fraction, the extent of association and the average molecular weight calculated on the basis of Stockmayer's postgel picture. The number average has again discontinuous slope across the gel point, while the weight average remains divergent in the postgel regime.

but there still remains divergence in opinions. One series of studies postulate [89] the existence of short crystallizable stereoregular segment sequences on polymer chains, even if they are atactic, that are responsible for the formation of microcrystalline junctions. Another studies [4, 90] propose that cross-linking takes place by specific interaction such as formation of stoichiometric compounds involving solvent molecules. If such complex formation is the mechanism of cross-linking, the gelation temperature should not show a steadily increasing function of the polymer concentration, but should show a maximum at a certain concentration [90]. Existence of specific interaction was later suggested by light scattering study of at-PS dilute solution in toluene-CS_2 mixture [91].

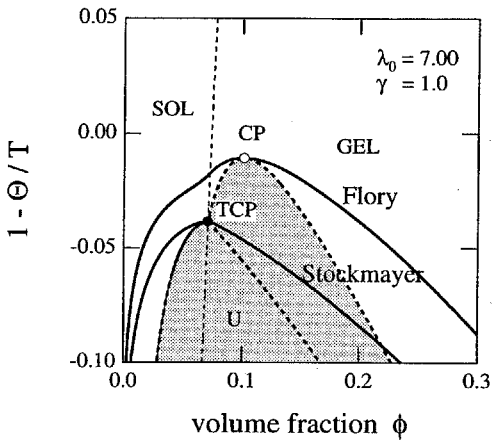

Figure 1.15. Comparison of the theoretical phase diagrams for low molecular-weight ($n = 1$) trifunctional ($f = 3$) molecules calculated by Flory's treatment (upper lines) and Stockmayer's treatment (lower lines) of the postgel regime for the same association constant. Flory's treatment allows cycle formation within the gel network, so that phase separation between dilute gel with only a few cycles and concentrated gel with many cycles with a critical solution point (white circle indicated by CP) is possible in the postgel regime. (Reprinted with permission of Ref.[14]. Copyright 2002, Jap. Soc. Polym. Sci.)

3.3 Multiple Association

Most thermoreversible gels of polymers and biopolymers have cross-link junctions connecting polymer segments belonging to several distinct chains (*multiple junctions*). For instance, gelation by micro-crystallization of the chain segments, by ionic aggregation, and by hydrophobic association of special groups attached on the polymer chains, all belong to this important category [4, 5]. In some biopolymer gels, triple helices serve as extended cross-link junctions.

Among these, *associating polymers* are very important, because they form ultraweak networks in water. Associating polymers are water-soluble polymers carrying hydrophobic groups on the backbone or on the chain side [13, 92]. Typical model APs that have recently been the focus of study are water-soluble polymers partially modified by hydrophobic groups. One series of APs are based on poly(ethylene oxide) chains (PEO), being modified by short alkyl chains [93, 94, 95, 96, 97, 98, 99], propyrene oxide (or butylene oxide) chains [100] and fluorocarbon chains [101, 102, 103, 104]. Hydrophobes are either periodically or randomly attached on a polymer chain. The simplest one is a telechelic poly-

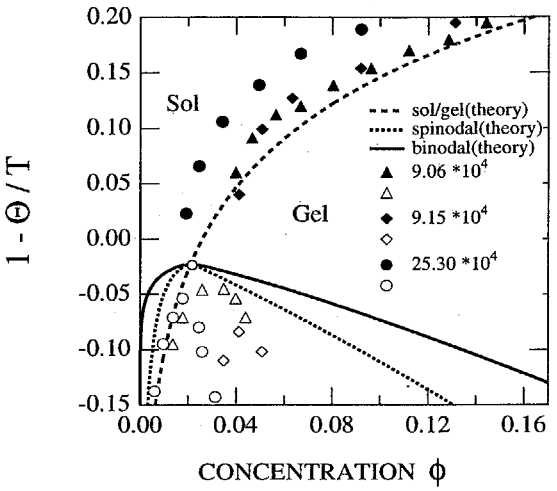

Figure 1.16. Phase diagram of atactic polystyrene in carbon disulfide. Thermoreversible gelation coexist with phase separation. Theoretical sol/gel transition line (broken line), binodal (solid line) and spinodal (dotted line) are drawn. Temperature is measured by the reduced temperature $\tau \equiv 1 - \Theta/T$ with the theta tempearature $\Theta = -70°C$. Experimental data of the gel points (black symbols) and cloud points (white symbols) are shown for three different molecular weights. Theoretical calculation is fitted to the data for $M = 9.06 \times 10^4$. (Reprinted with permission of Ref.[14]. Copyright 2002, Jap. Soc. Polym. Sci.)

mer carrying two hydrophobes at the chain ends. Another series of APs are based on cellulose derivatives. Some examples are ethyl hydroxyethyl cellulose (EHEC) [105, 106, 107] and hydroxypropyl methyl cellulose (HPMC) [108, 109]. Polyelectrolytes partially modified by hydrophobic groups have also been intensely studied [110, 111, 112, 113, 114].

In this section, we attempt to extend our theory from pairwise association to more general multiple association. As a model solution, we consider a mixture of associative molecules in a solvent. Molecules are distinguished by the number f of the associative groups they bear, each group being capable of taking part in the junctions with variable multiplicity which may bind together any number k of such groups [115, 116, 117]. We include $k = 1$ for unassociated groups. We allow junctions of all multiplicities to coexist, in proportions determined by the thermodynamic equilibrium conditions. In order to incorporate polydispersity in the functionality, we allow the number f of associative groups

to vary. Such polydispersity in the functionality of polymers is essential when associative groups are activated by the conformational transition of polymers as in biopolymer gels. In such cases, the functionality f is not a fixed number but changes depending upon temperature, concentration and other environmental parameters.

Let n_f be the number of the statistical segments on an f-functional primary molecule, and let N_f be the total number of molecules in the solution. The weight fraction w_f of the associative groups carried by the molecules with specified f relative to the total number of associative groups is given by

$$w_f = fN_f / \sum fN_f. \tag{3.58}$$

The number- and weight-average functionality of the primary molecules are then defined by

$$f_{\rm n} \equiv (\sum w_f/f)^{-1}, \tag{3.59a}$$

$$f_{\rm w} \equiv \sum f w_f. \tag{3.59b}$$

The volume fraction of f-functional molecules is given by $\phi_f = n_f \nu_f$, where $\nu_f \equiv N_f/\Omega$ is their number density, and the total volume fraction by $\phi = \sum_f \phi_f$.

In thermal equilibrium, the solution has a distribution of clusters with the population distribution fixed by the equilibrium conditions. Following the notation used by Fukui and Yamabe [115], we define a cluster of type $(\mathbf{j};\mathbf{l})$ to consist of j_k junctions of multiplicity k $(k = 1,2,3,...)$ and l_f molecules of functionality f $(f = 1,2,3,...)$. The bold letters $\mathbf{j} \equiv \{j_1, j_2, j_3, ...\}$ and $\mathbf{l} \equiv \{l_1, l_2, l_3, ...\}$ denote the sets of indices. An isolated molecule of functionality f, for instance, is indicated by $\mathbf{j}_{0f} \equiv \{f, 0, 0, ...\}$, and $\mathbf{l}_{0f} \equiv \{0, ..., 1, 0, ...\}$. (The f-th number is unity, others are zero.)

Let $N(\mathbf{j};\mathbf{l})$ be the number of $(\mathbf{j};\mathbf{l})$-clusters in the system. Then their number density is given by $\nu(\mathbf{j};\mathbf{l}) = N(\mathbf{j};\mathbf{l})/\Omega$, and their volume fraction is given by

$$\phi(\mathbf{j};\mathbf{l}) = \left(\sum_{f \geq 1} n_f l_f \right) \nu(\mathbf{j};\mathbf{l}). \tag{3.60}$$

The total volume fraction of the polymer component in the sol part is given by the sum over all possible cluster types

$$\phi = \sum_{\mathbf{j},\mathbf{l}} \phi(\mathbf{j};\mathbf{l}). \tag{3.61}$$

As in the preceding sections, we start from the standard reference state (polymers and solvent molecules being separated in hypothetical

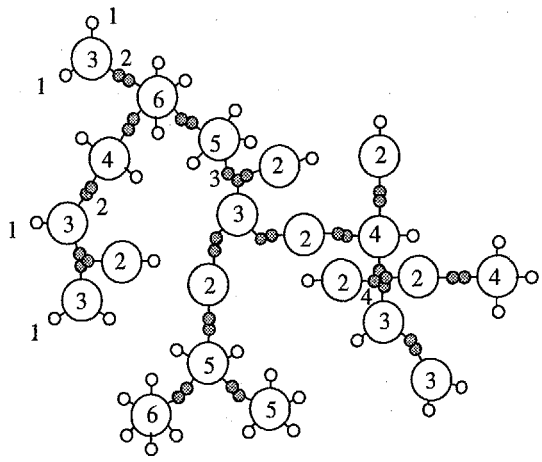

Figure 1.17. A cluster formed by multiple association. It is characterized by a set of vectorial indices **j** specifying the type of junctions and **l** specifying the type of molecules.

crystalline states). The free energy change on passing from this reference state to the final solution, at equilibrium with respect to cluster formation, is given by [116]

$$\beta\Delta F/\Omega = \phi_0 \ln \phi_0 + \sum_{\mathbf{j},\mathbf{l}} \nu(\mathbf{j};\mathbf{l})[\Delta(\mathbf{j};\mathbf{l}) + \ln \phi(\mathbf{j};\mathbf{l})] + \chi\phi_0\phi + \sum_f \nu_f^G \delta_f(\phi). \tag{3.62}$$

Here, the free energy change $\Delta(\mathbf{j};\mathbf{l})$ accompanying the formation of a $(\mathbf{j};\mathbf{l})$-cluster in a hypothetical undiluted amorphous state from the separate primary molecules in their standard states is defined by

$$\Delta(\mathbf{j};\mathbf{l}) \equiv \beta \left\{ \mu^\circ(\mathbf{j};\mathbf{l}) - \sum_f l_f \mu^\circ(\mathbf{j}_{0f};\mathbf{l}_{0f}) \right\}. \tag{3.63}$$

In the postgel regime where a cluster grows to a macroscopic network, the free energy has the last term for the gel part [12, 116].

Following the general strategy, we first derive chemical potentials of the clusters and solvent, and pose chemical equilibrium conditions

$$\Delta\mu(\mathbf{j};\mathbf{l}) = \sum_f l_f \Delta\mu(\mathbf{j}_{0f};\mathbf{l}_{0f}) \tag{3.64}$$

to find the cluster size distribution function written in terms of the volume fraction of the polymer chains that remain unassociated. Sub-

stituting the result back into the starting free energy (3.62), we find it in the form of (1.29), where the association part is given by

$$f_{\rm AS}(\{\phi\}) = \sum_f \frac{\phi_f}{n_f} \ln(\frac{\phi_{0f}}{\phi_f}) + 1 - \phi + \sum_f \frac{\phi_f}{n_f} - \nu^S. \tag{3.65}$$

Here, $\phi_{0f} \equiv \phi(\mathbf{j}_{0f}; \mathbf{l}_{0f})$ is the volume fraction of f-molecules that remain unassociated in the solution. The number of molecules and clusters possessing translational degree of freedom takes the form

$$\nu^S = \left(\sum_f \frac{\phi_f}{n_f} \right) / \bar{l}_{\rm n} + 1 - \phi. \tag{3.66}$$

To derive $\bar{l}_{\rm n}$ (the number-average DP of the clusters), we again apply classical tree statistics, but now augmented to suit for multiple association. We have recently presented a systematic method [118, 119] to calculate number- and weight-average DP of condensate polymers (aggregates). This method is based on the application of cascade process [120] to polycondensation of functional molecules. Derivation of the main result is straightforward but tedius, so that we describe here only the outline of the multiple cascade theory.

We first introduce the probability p_k for a randomly chosen associative group to be in the junction of multiplicity k. The total extent α of reaction is given by

$$\alpha \equiv \sum_{k \geq 2} p_k. \tag{3.67}$$

Then, $p_1 \equiv 1 - \alpha$ is the probability for an associative group to remain unassociated. This is equivalent to the normalization condition $\sum p_k = 1$. The cascade theory then uses the function $u(x)$ with regard to the junction. This function (referred to as *junction function*) is defined by

$$u(x) \equiv \sum_{k \geq 1} p_k x^{k-1}. \tag{3.68}$$

The number- and weight-average multiplicity of the junctions are defined by

$$\bar{\mu}_{\rm n} \equiv \left(\sum_k p_k / k \right)^{-1}, \tag{3.69a}$$

$$\bar{\mu}_{\rm w} \equiv \sum_k k p_k. \tag{3.69b}$$

The cascade theory of multiple association [118, 119] then gives for the number- and weight-average DP of polymer aggregates

$$\bar{l}_{\rm n}^{-1} = 1 - f_{\rm n}\int_0^1 xu'(x)dx = 1 - f_{\rm n}(1 - 1/\bar{\mu}_{\rm n}), \tag{3.70a}$$

$$\bar{l}_{\rm w} = 1 + \frac{f_{\rm n}(\bar{\mu}_{\rm w} - 1)}{1 - (f_{\rm w} - 1)(\bar{\mu}_{\rm w} - 1)}. \tag{3.70b}$$

From the weight average, the gel point turns out to be given by the condition

$$(f_{\rm w} - 1)(\bar{\mu}_{\rm w} - 1) = 1. \tag{3.71}$$

In the case of thermoreversible reaction we are now concerned, the probability p_k obeys the reaction equilibrium condition

$$\psi p_k/(\psi p_1)^k = K_k, \tag{3.72}$$

where $\psi \equiv \sum fN_f/\Omega$ is the number density of functional groups. Hence, p_k is given by

$$p_k = K_k \psi^{k-1} p_1^k. \tag{3.73}$$

We then assume the form $K_k = \lambda(T)^{k-1}\gamma_k$, where $\lambda(T) = \exp(-\Delta f_0/k_B T)$ is the association constant (Δf_0 being the binding free energy), and γ_k includes the free energy due to the existence of the surface on the micellar junction. Substituting this form of p_k into the normalization condition, we find

$$\lambda(T)\psi = z\tilde{u}(z), \tag{3.74}$$

where the function $\tilde{u}(z)$ to be used to characterize the junctions is defined by

$$\tilde{u}(z) \equiv \sum_{k\geq 1} \gamma_k z^{k-1}, \tag{3.75}$$

by the parameter z defined by

$$z \equiv \lambda(T)\psi p_1 = \lambda(T)\psi(1 - \alpha). \tag{3.76}$$

This gives the concentration of the associative groups that remain unassociated in the solution (multiplied by the association constant). From (3.74) that relates the parameter z (and hence reactivity α) with the given polymer concentration ϕ, we can find $\bar{\mu}_{\rm n}$ and $\bar{\mu}_{\rm w}$ as functions of the temperature and concentration. Hence, we find the free energy. The gel point condition (3.71) is transformed into the equation

$$(f_{\rm w} - 1)z\tilde{u}'(z)/\tilde{u}(z) = 1. \tag{3.77}$$

The multiplicity of the junctions is in principle determined automatically by the equilibrium requirement for a given associative interaction. In the case of hydrophobic interaction, the chain length of a hydrophobe, the strength of water-hydrophobe interaction, the geometric form of an aggregate, and other factors determine the association constant $\lambda(T)$ and the junction multiplicity k. For practical treatment, we avoid complexity in finding the precise form of the coefficients γ_k, and hence distribution of the multiplicity, but instead, we introduce model junctions [116].

In one of the practical models in commmon use, multiplicities lying in a certain range covering from $k = k_{min}$ to k_{max} are equally allowed (*mini-max junction*). We have

$$k = 1 \quad \text{(free)}, \qquad k = k_{min}, k_{min}+1, ..., k_{max} \quad \text{(associated)}. \tag{3.78}$$

The junction function takes the form

$$\tilde{u}(z) = 1 + \sum_{k=k_{min}}^{k_{max}} z^{k-1} = 1 + (z^{k_{min}-1} - z^{k_{max}})/(1-z). \tag{3.79}$$

Such assumption of the limited range can be, to some extent, justified in the case of micelles of hydrophobic chains [117].

When only a single value is allowed, i.e., $k_{min} = k_{max} \equiv k$, we call the model *fixed multiplicity model*. Thus, for $k = 2$, fixed multiplicity model reduces to pairwise association. The above normalization relation for the fixed multiplicity model of monodisperse polymers (f and n definite) is given by

$$\lambda(T)\phi/n = \alpha^{1/(k-1)}/f(1-\alpha)^{k/(k-1)}, \tag{3.80}$$

in terms of the extent α of association to the (scaled) polymer concentration. The gel point condition (3.77) gives $(f-1)(k-1)\alpha = 1$ and hence

$$\alpha^* \equiv 1/(f-1)(k-1) \tag{3.81}$$

leading to the critical concentration

$$\lambda(T)\phi^*/n = (f-1)(k-1)/f[(f-1)(k-1)-1]^{k/(k-1)}, \tag{3.82}$$

where ϕ^* is the volume fraction of the polymer at the gel point.

Figure 1.18 plots the reduced concentration $\lambda(T)\phi^*/n$ at the gel point as functions of the junction multiplicity. The functionality is changed from curve to curve. For bifunctional molecules $f = 2$, at least multiplicity 3 is necessary for gelling. The gelation concentration monotonically decreases with multiplicity. For the functionality higher than 2, however, there is an optimal multiplicity for which gelation is easiest. In

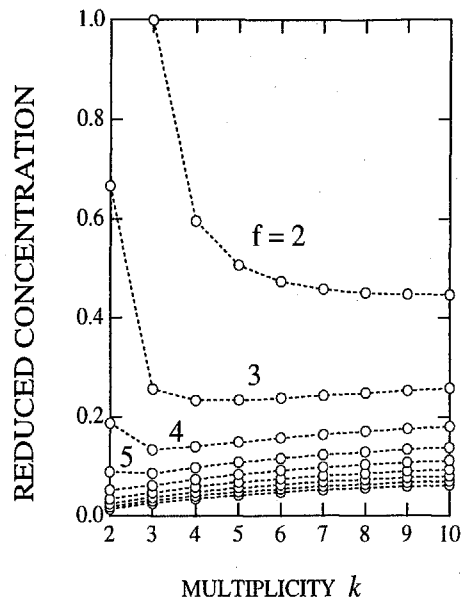

Figure 1.18. The reduced concentration $\lambda(T)\phi^*/n$ at the gel point plotted against the junction multiplicity. The functionality is varied from curve to curve. For bifunctional case of $f = 2$, it is a monotonically decreasing function, while for f larger or equal to 3 it has a mimimum at a certain multiplicity, where gelation becomes easiest.

such cases, growth of the networks becomes difficult with increase in the number of branches at the junctions.

Figure 1.19 shows the shift of phase diagrams with increase in the multipliicity for bifunctional molecules. Sol/gel transition line (thick broken lines), binodals (thin broken line) and spinodals (solid lines) are drawn for a fixed multiplicity within Flory's postgel treatment. Above a certain critical multiplicity ($k = 5$ in the Figure) two critical solution points merge into one, and phase diagram changes from CEP type to TCP type.

3.4 Structure of the Networks with Multiple Junctions

On passing the gel point, networks appear and coexist with finite clusters. The structure of a network can be studied from two different viewpoints: local viewpoint and global one. The local structure of a network focuses on the structure of each network junction, including its multiplicity, sequence length, degree of chain packing, etc., while the

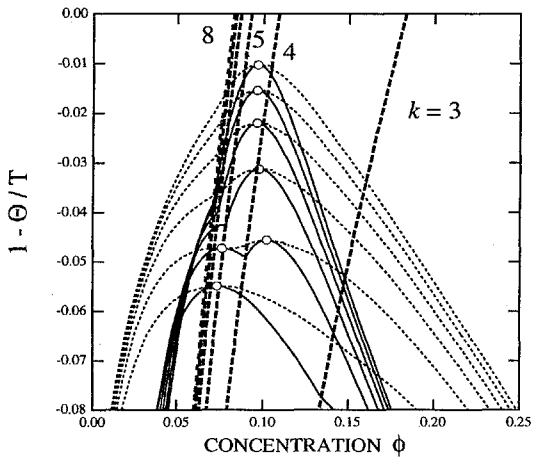

Figure 1.19. Sol/gel transition lines (thick broken lines), binodals (thin broken lines) and spinodal lines (solid lines) of bifunctional ($f = 2$) polymers with $n = 100$, $\lambda_0 = 10.0$ for association with fixed multiplicity ($k_{min} = k_{max} \equiv k$). Multiplicity k is changed from 3 to 8. The transition line shifts to high temperature and low concentration region with the multiplicity. Gelation is easier for larger multiplicity. (Reprinted with permission of Ref.[14]. Copyright 2002, Jap. Soc. Polym. Sci.)

global structure treats topological connectivity of the network as a whole, paying special attention to the *cycle rank* (number of independent loops), number of *elastically effective chains*, number of *dangling ends*, average *path number* of junctions, etc. Studies from such different viewpoints are complementary to each other, and both are necessary.

3.4.1 Local Structure of Networks — Augmented Eldridge-Ferry Method —. When an associative group on a chain involves ζ sequential repeat units, we can write the standard free energy change as $\Delta f_0 = \zeta(\Delta h - T\Delta s)$. By taking the logarithm of the gelation concentration (3.82), we find an important relation

$$\ln \phi^* = \zeta \frac{\Delta h}{k_B T} + \ln[\frac{(f-1)(k-1)n}{f\{(f-1)(k-1)-1\}^{k/(k-1)}}] - \zeta \frac{\Delta s}{k_B}. \qquad (3.83)$$

We can find multiplicity k and sequence length ζ by comparing this relation with the experimental sol/gel transition concentration (see Figure 1.20) [121]. For the hydrophobes on associating polymers, the enthalpy Δh of a cross-link is found because ζ is known from the number of carbons in a hydrophobe. For the fringed micellar micro-crystalline junction formed by homopolymers, each ζ sequence of repeat units along a chain surves as a functional group for cross-linking. In such a case, a polymer

chain is regarded as carrying roughly $f = n/\zeta$ functional groups. Since we have large n, and hence large f, we can neglect 1 compared to n or f, and led to an equation

$$\ln c^* = \zeta \frac{\Delta h}{k_B T} - \frac{1}{k-1} \ln M + constant \tag{3.84}$$

for micro-crystalline gels, where weight concentration c^* has been substituted for the volume fraction. This equation enables us to find ζ and k independently. For the special case of pairwise association $k = 2$, this equation reduces to the conventional Eldridge-Ferry equation [122].

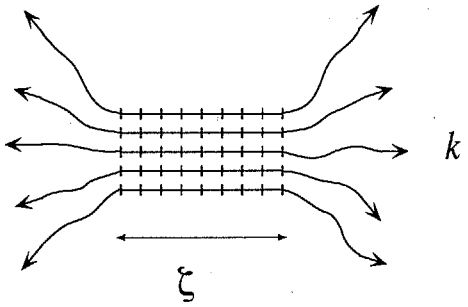

Figure 1.20. Micellar junction consisting k chains combined together by the monomer sequences of length ζ.

Let us plot $\ln c^*$ against $10^3/T + \ln M$. Then the slope $-B$ of the line at constant T gives $-1/(k-1)$, while the slope $-A$ of the line at constant M gives

$$\zeta = \frac{10^3 k_B}{|\Delta h|} A = \frac{10^3 R}{|(\Delta h)_{mol}|} A, \tag{3.85}$$

where $(\Delta h)_{mol}$ is the enthalpy of bonding per mole of the repeat units, and R the gas constant. We have applied this method to experimental data on the gel melting curves of several thermoreversible gels [123, 124].

As an example of such analysis, we show in Figure 1.21 the result for the gelation of poly(vinyl alcohol)(PVA) in water [123]. PVA is known to be a typical crystalline polymer, but it also gels in aqueous solution under large supercooling. There are several pieces of experimental evidence that the cross-links are formed by partial crystallization of the polymer segments in which syndiotactic sequence dominates, while subchains connecting the junctions consist mainly of atactic non-crystalline sequences on PVA chains. The micro-crystals at the junctions are supposed to be stabilized by hydrogen bonds between the hydroxy groups. We plot the

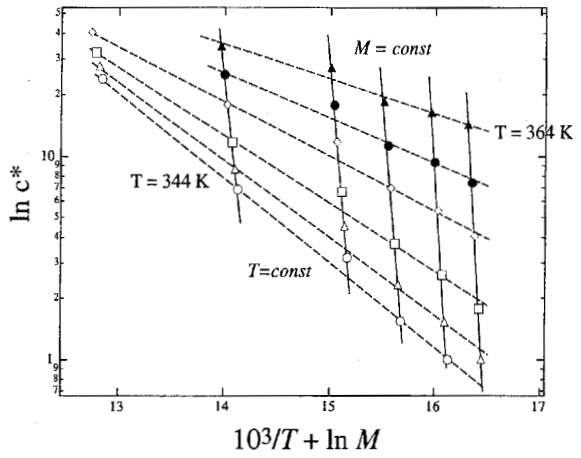

Figure 1.21. Augmented Eldridge-Ferry plot applied to the gel melting concentration of poly(vinyl alcohol)/water. Dotted lines show the gel melting concentration at constant temperature, while thin straight lines show those at constant molecular weight. (▲)91°C; (●) 87°C; (◇) 83°C; (□) 78°C; (△) 74°C; (○) 71°C. (Reprinted with permission of Ref.[123]. Copyright 1996, ACS.)

gel melting temperature (for a given concentration) found from differential scanning calorimetry (DSC) and visco-elastic measurements for PVA with different molecular weights covering the range from 2×10^4 to 8×10^5 in various concentrations [124]. The gel melting temperature $T_{\rm m}$ is estimated from the temperature at which the DSC heating curve shows an endotherm peak. The slope of the solid lines in Figure 1.21 with constant molecular weight gives $-A = 13.43$ almost independently of their molecular weights. Hence we find $\zeta = 26.7$ kcal/mol/$|(\Delta h)_{mol}|$. If we use the heat of fusion $(\Delta h)_{mol} = 1.64$ kcal/mol in the bulk crystal, we find $\zeta = 16.3$. On the other hand, the slope of the dotted lines with constant temperature depends on the temperature. At the highest temperature $T = 91$ °C in the measurement, it is -0.38, while it gives a larger value -0.9 at $T = 71$ °C. The multiplicity is estimated to decrease from 3.6 for high-temperature melting to 2.1 for low-temperature melting, suggesting a very thin junction structure. From thermodynamic stability of the junctions it is natural that a gel which melts at lower temperature has thinner junctions.

3.4.2 Global Structure of Networks — Elastically Effective Chains —. To study visco-elastic properties of networks, we next find the number ν_{eff} of elastically effective chains [8, 125]. The elas-

tically effective chains are those chains that transmit stress when the network is deformed by external force. They are related to the topological structure of the network. Let us first specify the type of junctions from their connection paths to the network matrix [121]. A junction of multiplicity k that is connected to the network matrix through i paths is referred to as an (i,k)-junction. Let $\mu_{i,k}$ be the number of junctions in the network specified by the type (i,k) for $0 \leq i \leq 2k$ and for $k = 1,2,3,4,\cdots$. The total number of junctions with multiplicity k is given by

$$\mu_k = \sum_{i=0}^{2k} \mu_{i,k}. \tag{3.86}$$

To find the number of elastically effective chains, we next employ the criterion introduced by Scanlan [126] and Case [127]. It assumes that only subchains connected at both ends to junctions carrying at least *three paths* to the gel are elastically effective. We thus have $i, i' \geq 3$ for an effective chain. A junction with one path $(i = 1)$ to the gel unites a group of subchains dangling from the network matrix whose conformations are not affected by an applied stress. A junction with two paths $(i = 2)$ to the gel merely extends the length of an effective subchain. We may call a junction with $i \geq 3$ an *elastically effective junction.* An effective chain is defined as a chain connecting two effective junctions at its both ends. We thus find

$$\mu_{eff} = \sum_{k=2}^{\infty} \sum_{i=3}^{2k} \mu_{i,k} \tag{3.87}$$

for the number of elastically effective junctions, and

$$\nu_{eff} = \frac{1}{2} \sum_{k=2}^{\infty} \sum_{i=3}^{2k} i\mu_{i,k} \tag{3.88}$$

for the number of elastically effective chains. These numbers can be explicitly written in terms of the cascade junction function $u(x)$ defined by (3.68). Specifically for monodisperse polymer chains with a fixed functionality f, the number of elastically effective chains in a unit volume of the solution takes the form

$$\nu_{eff} = \frac{1}{2}(f\nu\alpha)[(\zeta_1 + 2\zeta_2)(1 - \theta(\zeta_0)) - {\zeta_1}^2\theta'(\zeta_0)], \tag{3.89}$$

where ν is the total number density of chains, α the extent of association (3.67), the function $\theta(x)$ is the associated part of the junction function defined by the equation $u(x) \equiv 1 - \alpha + \alpha\theta(x)$, and ζ_i is the probability that a randomly chosen unassociated functional group to be connected

to the matrix of the gel network through the number i of paths [121]. These probabilities are written in terms of the solution ζ_0 of the algebraic equation

$$x = u(x)^{f-1} \tag{3.90}$$

that is smaller than unity (see reference [121] for details).

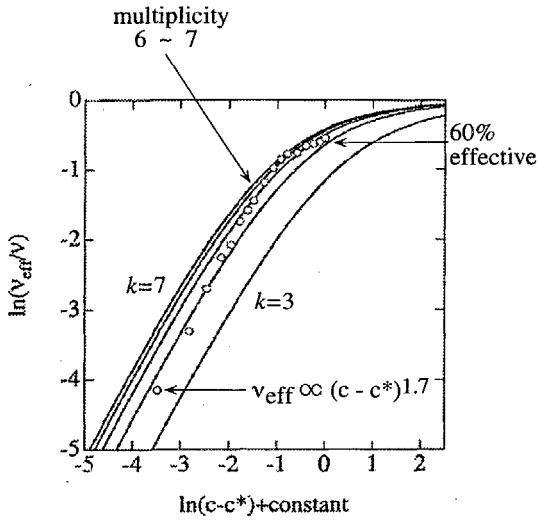

Figure 1.22. The number of elastically effective chains as a function of the polymer concentration. Experimental data of the HEUR 16C/35K are compared with theoretical calculation. In the theoretical calculation the junction multiplicity k is changed from curve to curve. (Reprinted with permission of Ref.[121]. Copyright 1996, ACS.)

These topological relations hold for arbitrary networks. Their advantage lies in the fact that, by combinatorial counting, we can actually find $\mu_{i,k}$ as a function of the degree α of association [128]. In our study, the degree α is found as a function of the temperature and concentration through the relation (3.74), so that all topological numbers described above can be calculated as functions of the temperature and concentration [121]. These curves can be compared with the experimental data on the high frequency dynamic modulus measured by Annable et al. [93] Their experimental data for HEUR C16/35K (PEO end-capped with $C_{16}H_{33}$, molecular weight 35,000) are compared with our theoretical calculation [121] for $f = 2$ in Figure 1.22. We have chosen as $c^* = 1.0\%$ for the weight concentration at gelation. With this gel concentration, the scaling power at the critical region gives $t = 1.6$, close to the percolation value [129]. But since this power depends sensitively on the way

we choose c^*, more detailed experimental examination in the critical region is eagerly required. In fitting the data, we have horizontally shifted the experimental data because of the temperature pre-factor $\lambda(T)$ and also because of the difference in the unit of the polymer concentration. Although fitting by a single theoretical curve is impossible due to the existence of polydispersity in the multiplicity, our theory produces a good result over a wide range of the concentration with multiplicity ranging from 6 to 8. It turns out that about 60% of chains are elastically effective at the limit of high concentration.

3.5 Mixtures of Associative Molecules — Gelation with Co-Networks —

In biological and medical science, thermoreversible gels consisting of more than two species of molecules or polymers are very important for controlling the crosslink structure. For example, it has been suggested that the repeated sol/gel transition of actin, controlled by actin-binding protein (ABP), drives motions of individual biological cells [130]. In this ternary system (actin, ABP and water), ABP works as a cross-linker of the actin filaments. In the food industry, biopolymer mixtures in which either single or multiple ingredients form networks have many important applications, and have been a focus of intensive experimental study [131, 132].

To study thermoreversible formation of mixed networks, we first consider a model mixture of reactive molecules $\mathrm{R}\{\mathrm{A}_f\}$ and $\mathrm{R}\{\mathrm{B}_g\}$, each carrying the number f of A-groups and g of B-groups. Another important cases where each molecule carries both of the two species A and B (*co-associating polymer*) have recently been studied [118, 133]. We allow multiple association of both groups, but first consider simpler case of pairwise association [16, 134]. The strength of the bonds can be expressed by the three association constants eq.(2.1). By the relative strength of these constants, let us now classify the types of association into the following fundamental three categories [16]:

(i) *Interpenetrating Polymer Networks* (IPN) — Reactive groups A and B form bonds within the same species, but do not form between different species, i.e., $\lambda_{AB} = 0$. We refer to this case as A·A/B·B.

(ii) *Alternating Polymer Networks* (APN) — Bonds are allowed only between different species, i.e., $\lambda_{AA} = \lambda_{BB} = 0$. We refer to this case as A·B. Because the clusters (of finite or infinite size) formed are in general multi-block copolymers, the system may undergo mi-

crophase separation. Hence, macrophase separation, microphase separation and gelation interfere with each other.

(iii) *Randomly Mixed Networks* (RMN) — If the strengths of associative forces in all three combinations are of the same order, cluster formation progresses randomly. The resultant networks can be regarded as macroscopic random block-copolymers.

We now extend this classification to suit for multiple association. For multiple association, it is convenient to classify from the mixing properties *inside* the junctions. To specify a multiple junction precisely, let us introduce a set of integers (k_1, k_2), where k_1 is the number of A groups it contains, and k_2 is that of B groups [118, 119]. The cascade junction functions then take the form

$$u_A(x,y) = \sum_{k_1\geq 1, k_2\geq 0} p_{k_1,k_2} x^{k_1-1} y^{k_2}, \tag{3.91a}$$

$$u_B(x,y) = \sum_{k_1\geq 0, k_2\geq 1} q_{k_1,k_2} x^{k_1} y^{k_2-1}, \tag{3.91b}$$

for the junction which an arbitralily chosen A-group (and B-group) enters, where p_{k_1,k_2} is the probability for a randomly chosen A-group to be in the junction specified by the number (k_1, k_2), and q_{k_1,k_2} is the same for B-group. We have recently shown that the number density ν^S of the clusters and molecules that possess translational degree of freedom is given by

$$\nu^S = \frac{\phi}{n_A}\left\{1 - f\int_0^1 x u_A'(x)dx\right\} + \frac{1-\phi}{n_B}\left\{1 - g\int_0^1 y u_B'(y)dy\right\}, \tag{3.92}$$

where abbreviated notations $u_A(x) \equiv u_A(x,x)$ etc. for the diagonal elements have been used.

This result can be intuitively derived by stoichiometric consideration. Within the tree approxiamtion, the number of connected clusters is the same as the number of primary molecules minus total number of connecting bonds. The integral in (3.92) gives

$$\int_0^1 x u_A'(x)dx = \sum \frac{k_1+k_2-1}{k_1+k_2} p_{k_1,k_2} = 1 - \frac{1}{\bar{\mu}_A}, \tag{3.93}$$

and hence

$$\nu^S = \frac{\phi}{n_A}\left\{1 - f\left(1 - \frac{1}{\bar{\mu}_A}\right)\right\} + \frac{1-\phi}{n_B}\left\{1 - g\left(1 - \frac{1}{\bar{\mu}_B}\right)\right\}. \tag{3.94}$$

Here, the average multiplicity $\bar{\mu}_A$ and $\bar{\mu}_B$ of the mixed junctions are defined by

$$\bar{\mu}_A^{-1} \equiv \sum p_{k_1,k_2}/(k_1+k_2), \quad \text{and} \quad \bar{\mu}_B^{-1} \equiv \sum q_{k_1,k_2}/(k_1+k_2). \tag{3.95}$$

Since the number of unreacted A-groups and that of B-groups are given by $\psi_A p_{1,0}$, and $\psi_B q_{0,1}$, reaction equilibrium condition for an A-group joining in a (k_1, k_2) junction, is given by

$$\frac{\psi_A p_{k_1,k_2}}{(\psi_A p_{1,0})^{k_1}(\psi_B q_{0,1})^{k_2}} = K^{(A)}_{k_1,k_2}, \tag{3.96}$$

where $K^{(A)}_{k_1,k_2}$ is the reaction equilibrium constant. Similar relation holds also for B-groups. Now we assume as usual that the equilibrium constant takes the form

$$K^{(A)}_{k_1,k_2} = \gamma^{(A)}_{k_1,k_2} \lambda_A(T)^{k_1-1} \lambda_B(T)^{k_2}, \tag{3.97}$$

where

$$\lambda_\alpha(T) = \exp(-\Delta f_\alpha / k_B T), \qquad \text{for } \alpha = A, B, \tag{3.98}$$

are the association constants written in terms of the free energy Δf_α required for binding a reactive group of the type α into the junction. The coefficient $\gamma^{(A)}_{k_1,k_2}$ gives correction due to the existence of the surface of micellar junction [116]. Similar formulae for $K^{(B)}_{k_1,k_2}$ are assumed.

Substituting the results into the cascade junction functions, we find

$$u_A(x,y) = p_{1,0} \sum_{k_1 \geq 1, k_2 \geq 0} \gamma^{(A)}_{k_1,k_2} (z_A x)^{k_1-1} (z_B y)^{k_2} \tag{3.99}$$

by using new variables $z_A \equiv \lambda_A \psi_A p_{1,0}$ and $z_B \equiv \lambda_B \psi_B q_{0,1}$. These z parameters have physical meanings of the number densities of reactive groups (times association constant) that remain unassociated in the system. We next define $\tilde{u}$ function by the sum in (3.99) as

$$\tilde{u}_A(x,y) \equiv \sum_{k_1 \geq 1, k_2 \geq 0} \gamma^{(A)}_{k_1,k_2} x^{k_1-1} y^{k_2}, \tag{3.100}$$

and similar equation for $\tilde{u}_B$. Since $u_A(1,1) = 1$, we find parameters z_A and z_B satisfy the coupled equations

$$\lambda_A \psi_A = z_A \tilde{u}_A(z_A, z_B), \tag{3.101a}$$

$$\lambda_B \psi_B = z_B \tilde{u}_B(z_A, z_B). \tag{3.101b}$$

By solving these equations with respect to z's, we find them as functions of given total number of reactive groups in a unit volume. Solution

properties, the gel point, etc. can be studied by subsituting the result into chemical potentials, the weight-average molecular weight etc.

For pairwise association, We have only to assume $p_{1,0} = 1 - (\alpha + p), p_{1,1} = p, p_{2,0} = \alpha$ and $q_{0,1} = 1 - (\beta + q), q_{1,1} = q, q_{0,2} = \beta$, where α is the reaction probability of an A-group with A-group, p is that with B-group, while β is the reaction probability of a B-group with B-group, q is that with A-group. We show here in Figure 1.23(a),(b) typical phase diagrams[16] of alternately cross-linked networks in a symmetric case ($n_A = n_B = 10$, $f = g = 3$, $\lambda_0 = 1.0$). The dimensionless binding energy γ, eq.(2.5) between the functional groups on A-chains and B-chains is different. Thick solid lines show the sol/gel transition lines, thin dashed lines binodal, thin solid lines spinodal, and white circles the critical solution point. The gel region is indicated by the horizontal lines, and the unstable region (U) is shaded. For small γ, the gel region lies inside the unstable region, so that a stable homogeneous gel is not expected. In Figure 1.23 (a), the population of hetero-clusters becomes so large at low temperatures that a reentrant homogeneous phase appears, and as a result, a new critical solution point appears lying on the sol/gel transition line. With a slight increase in γ, the two critical solution points lying at $\phi = 0.5$ merge into a single one. With further increase in γ, the gel region grows and the miscibility gap is completely separated near around the stoichiometric concentration $\phi = 0.5$ (in the symmetric case) by the existence of mixed clusters.

As for mixed networks with multiple junction, Clark et al. [131], for instance, studied composite aqueous gels consisting of thermoreversible cold-setting gelling components such as agarose and gelatin by electron- and optical microscopy. They reported that their micrographs appeared quite similar to those observed in a number of synthetic interpenetrating networks [135, 136], and showed phase separation into the two polymer networks with possible phase inversion at a certain mixture composition. Durrani et al. [137, 138] derived a phase diagram for the ternary amylopectin-gelatin-D_2O mixture in the sol state by the use of Fourier transformed infrared microspectroscopy.

Formation of mixed networks may also be used to modify the rheological properties of aqueous polymer solutions. For instance, recently it was experimentally demonstrated [139] that the viscosity of mixtures of the two species of polymers, poly(N-isopropylacrylamide) and hydrophobically modified poly(sodium acrylate) in aqueous solution becomes several orders of magnitude higher than is achieved without hydrophobic modification. Possible mechanism of heteropolymer cross-linking between the hydrophobes on the different species, followed by network formation by the hydrophobic aggregation of molecules, was proposed [139].

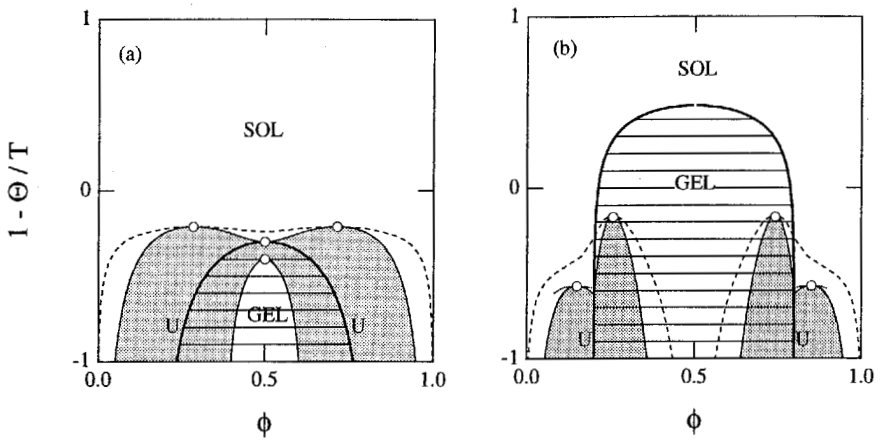

Figure 1.23. Phase diagrams of a alternately cross-linked network in the mixture of low molecular-weight trifunctional molecules (Flory's treatment); $n_A = n_B = 10$, $f = g = 3$, $\lambda_0 = 1.0$. Association constants γ is changed with other parameters being fixed: (a) $\gamma = 1.9926$, (b) $\gamma = 5.0$. The sol/gel transition lines (thick solid lines), binodal (thin dashed line) and spinodal (thin solid line) are shown. The postgel region is indicated by thin horizontal lines. The shaded regions indicated by letter U, are unstable regions. The open circles show critical solution points. The gel region lies inside the spinodal for small values of association constant as in (a), but in the case of strong association as shown in (b), the miscibility gap splits into two separate pieces, and the gel region is stabilized. The alternating network works as the solvilizer in this case due to their amphiphilic nature. The critical points stay inside the gel region so that phase separation into two gels with different concentrations, and hence different cross-link density, is possible. (Reprinted with permission of Ref.[16]. Copyright 1999, ACS.)

Theory presented in this section for treating binary mixtures with heteromolecular association is directly applicable to other important systems. For instance, when polymer-polymer association and polymer-water association coexist as seen in aqueous biopolymer solutions, we have a mixture of $R\{A_f\}$ and $R\{B_1\}$ with A·A and A·B bonds, competition between hydration and cross-linking takes place. As a result, the solution gels at high temperature (*inverted gelation*). Interaction of hydrophobically modified water-soluble polymers with added surfactant molecules is another important example. In this case, hydrophobes of the surfactant molecules strongly interact with those on the polymers, and form mixed micelles. The polymer network is modified by the concentration of the added surfactant, leading to interesting rheological behavior. Readers may easily find other potential applications of the

present theory to complex associating polymer solutions of industrial importance.

4. SUMMARY

We have presented an outline of the theoretical scheme to study molecular association and thermoreversible gelation in polymer solutions and mixtures. Thermodynamic nature of the sol/gel transition, interference with phase separation, structure of the network junctions, path connectivity in the network have been studied on the basis of the multiple tree statistics combined with classical lattice-theoretical polymer solutions. The present studies have mainly focused on the gelation of water-soluble associating polymers driven by hydrophobic aggregation, but find many applications to other types of gels such as those driven by hydrogen bonds, micro-crystallization, helix formation etc. We close in hoping that, after reading this section, readers try to find phase diagrams of their own systems in the framework of the present theory.

References

[1] Clark, A.H. and Ross-Murphy, S.B., *Ad. Polym. Sci.* **1987**, *83*, 57.

[2] Russo, P.S., *"Reversible Polymeric Gels and Related Systems"*, ACS Symposium Series **1987**, *350*.

[3] Kramer, O., *"Biological and Synthetic Polymer Networks"*, Elsevier Applied Science, London and New York **1988**.

[4] Guenet, J.M., *"Thermoreversible Gelation of Polymers and Biopolymers"*, Academic Press, Harcourt Brace Jovanovich Publishers **1992**.

[5] te Nijenhuis, K., *Ad. Polym. Sci.* **1997**, *130*, 1.

[6] Flory, P.J., *J. Chem. Phys.* **1944**, *12*, 425.

[7] Huggins, M.L., *J. Chem. Phys.* **1942**, *46*, 151.

[8] Flory, P.J., *"Principles of Polymer Chemistry"*, Cornell University Press **1953**.

[9] Koningsveld, R., Stockmayer, W.H. and Nies, E., *"Polymer Phase Diagrams"*, Oxford University Press **2001**.

[10] Tanaka, F., *Macromolecules* **1989**, *22*, 1988.

[11] Tanaka, F. and Matsuyama, A., *Phys. Rev. Lett.* **1989**, *62*, 2759.

[12] Tanaka, F., *Macromolecules* **1990**, *23*, 3784; 3790.

[13] Tanaka, F. and Koga, T., *Bull. Chem. Soc. Jpn* **2001**, *74*, 201.

[14] Tanaka, F., *Polym. J.* **2002**, *74*, 479.

[15] Šolc, K., *Macromolecules* **1970**, *3*, 665.

[16] Tanaka, F. and Ishida, M., *Macromolecules* **1999**, *32*, 1271.

[17] Shultz, A.R., and Flory, P.J., *J. Am. Chem. Soc.* **1953**, *75*, 3888; 5631.

[18] Tanaka, F., Ishida, M. and Matsuyama, A., *Macromolecules* **1991**, *24*, 5582.

[19] Kielhorn, L. and Muthukumar, M., *J. Chem. Phys.* **1997**, *107*, 5588.

[20] Tanaka, H. and Hashimoto, T., *Macromolecules* **1991**, *24*, 5398; 5713.

[21] Leibler, L., *Macromolecules* **1980**, *13*, 1602.

[22] Bates, F.S. and Fredrickson, G.H., *Ann. Rev. Phys. Chem.* **1990**, *41*, 525.

[23] Hornreich, R.M., Luban, M. and Shtrikman, S., *Phys. Rev. Lett.* **1975**, *35*, 1678.

[24] Haraguchi, M., Nakagawa, T. and Nose, T. *Polymer* **1995**, *36*, 2567.

[25] Haraguchi, M., Inomata, K. and Nose, T., *Polymer* **1996**, *37*, 3611.

[26] Inomata, K., Haraguchi, M. and Nose, T., *Polymer* **1996**, *37*, 4223.

[27] Lehn, J.-M., *"Supramolecular Chemistry—Concepts and Perspectives"*, VCH **1995**.

[28] Ciferri, C., *"Supramolecular Polymers"*, Marcel Dekker, Inc. **2000**.

[29] Kato, T., *Structure and Bonding* **2000**, *96*, 95.

[30] Jacobson, H. and Stochmayer, W.H., *J. Chem. Phys.* **1950**, *18*, 1600; **1950**, *18*,1607.

[31] Mayer, J.E. and Mayer, M.G., *"Statistical Mechanics"*, Chap.16, John Wiley & Sons, Inc. **1940**

[32] Truesdell, C., *Ann. Math.* **1945**, *46*, 144.

[33] Scott, R.L., *J. Phys. Chem.* **1965**, *69*, 261; **1967**, *71*, 352.

[34] Wheeler, J.C. and Pfeuty, P., *Phys. Rev. Lett.* **1981**, *46*, 1409.

[35] Wheeler, J.C. and Pfeuty, P., *Phys. Rev.* **1981**, *A24*, 1050.

[36] Wheeler, J.C. and Pfeuty,,P., *J. Chem. Phys.* **1981**, *74*, 6415.

[37] Dudowicz, J., Freed, K. and Douglas, J.F., *J. Chem. Phys.* **1999**, *111*, 7116; **1999**, *112*, 1002.

[38] Terech, P. and Weiss, R.G., *Chem. Rev.* **1997**, *97*, 3133.

[39] Tanaka, F. and Ishida, M., *Macromolecules* **1997**, *30*, 1836.

[40] Tanaka, F., *Macromolecules* **2004**, *37*, 605.

[41] Matsuyama, A. and Tanaka, F., *Phys. Rev. Lett.* **1990**, *65*, 341.

[42] Ruokolainen, J., ten Brinke, G., Ikkala, O., Torkkeli, M. and Serimaa, R., *Macromolecules* **1996**, *29*, 3409.

[43] Ruokolainen, J., Torkkeli, M., Serimaa, R., Vahvaselkä, S., Saariaho, M., ten Brinke, G. and Ikkala, O., *Macromolecules* **1996**, *29*, 6621.

[44] ten Brinke, G., Ruokolainen, J. and Ikkala, O., *Europhys. Lett.* **1996**, *35*, 91.

[45] ten Brinke G. and Ikkala, O., *Trends Polym. Sci.* **1997**, *5*, 213.

[46] Ruokolainen, J., Torkkeli, M., Serimaa, R., Komanschek, B.E., Ikkala, O. and ten Brinke, G., *Phys. Rev. E.* **1996**, *54*, 6646.

[47] Angerman, H.J. and ten Brinke, G., *Macromolecules* **1999**, *32*, 6813.

[48] Yashima, E., Matsushima, T. and Okamoto, Y., *J. Amer. Chem. Soc.* **1997**, *119*, 6345.

[49] Yashima, E., Maeda, K. and Okamoto, Y., *Nature* **1999**, *399*, 449.

[50] Maeda, K., Okada, S., Yashima, E. and Okamoto, Y., *J. Polym. Sci. Part A, Polym. Chem.* **2001**, *39*, 3180.

[51] Morino, K., Maeda, K., Okamoto, Y., Yashima, E. and Sato, T., *Chem. Eur. J.* **2002**, *8*, 5112.

[52] Anderson, G.R. and Wheeler, J.C., *J. Chem. Phys.* **1980**, *73*, 5778.

[53] Walker, J.S. and Vause, C.A., *Phys. Lett.* **1980**, *79A*, 421.

[54] Goldstein, R.E. and Walker, J.S., *J. Chem. Phys.* **1983**, *78*, 1942.

[55] Walker, J.S. and Vause, C.A., *Sci. Am.* **1987**, *256*, 90.

[56] Narayanan, T. and Kumar, A., *Phys. Rep.* **1994**, *249*, 135.

[57] Saeki, S., Kuwahara, N., Konno, S. and Kaneko, M., *Macromolecules* **1973**, *6*, 247; **1975**, *8*, 799.

[58] Saeki, S., Kuwahara, N., Nakata, M. and Kaneko, M., *Polymer* **1976**, *17*, 685.

[59] Dormidontova, E.E., *Macromolecules* **2002**, *35*, 987.

[60] Bekiranov, S., Bruinsma, R. and Pincus, P., *Phys. Rev. E* **1997**, *55*, 577.

[61] Bazuin, C.G., In *"Mechanical and Thermophysical Properties of Polymer Liquid Crystals"*, Chap.3, Brostow, W., Eds., Chapman & Hall, London **1998**.

[62] Bradfield, A.E. and Jones, B., *J. Chem. Soc.* **1929**, 2660.

[63] Jones, B., *J. Chem. Soc.* **1935**, 1874.

[64] Weygand, C., Gabler, R., *Z. Phys. Chem.* **1940**, *B46*, 270.

[65] Gray, G.W. and Jones, B., *J. Chem. Soc.* **1953**, , 4179.

[66] Brienne, M.-J., Gabard, J., Lehn, J.-M. and Stibor, I., *J. Chem. Soc. Chem. Comm.* **1989**, 1868.

[67] Kato, T. and Fréchet, J.M.J., *Macromolecules* **1989**, *22*, 3818.

[68] Maier, W., Saupe, A., *Z. Naturforsch.* **1958**, *13a*, 564; **1959**, *14a*, 882; **1960**, *15a*, 287.

[69] McMillan, W.L., *Phys. Rev.* **1971**, *A4*, 1238.

[70] Shoji, M. and Tanaka, F., *Macromolecules* **2002**, *35*, 7460.

[71] Cahn, J.W., *Trans. Metall. Soc.*, AIME **1968**, *242*, 166.

[72] Martin, J.W., Doherty, R.D. and Cantor, B., *"Stability of Microstructures in Metallic Systems"*, Sec.3.2, Cambridge Univ. Press **1997**.

[73] Olmsted, P.D., Poon, W.C.K., McLeish, T.C.B., Terrill, N.J. and Ryan, A.J., *Phys. Rev. Lett.* **1998**, *81*, 373.

[74] Flory, P.J., *Proc. Roy. Soc., London* **1956**, *A234*, 73.

[75] Miller, W.G., Kou, L., Tohyama, K. and Voltaggio, V., *J. Polym, Sci.: Polym. Symp.* **1978**, *65*, 91.

[76] Whittaker, E.T. and Watson, G.N., *"A Course of Modern Analysis"*, Chap.2, Cambridge Univ. Press **1969**.

[77] Tanford, C., *"The Hydrophobic Effect"*, Chap.7, John Wiley & Sons, Inc. **1980**.

[78] Candau, S.J., Hirsch, E. and Zana, R., *J. Phys. France* **1984**, *45*, 1263.

[79] Shikata, T., Hirata, H. and Kotaka, T., *Langmuir* **1987**, *3*, 1081; **1988**, *4*, 354.

[80] Hofmann, H. and Rehage, H., *Mol. Phys.* **1989**, *5*, 1225.

[81] Flory, P.J., *J. Am. Chem. Soc.* **1941**, *63*, 3091; **1941**, *63*, 3096.

[82] Stockmayer, W.H., *J. Chem. Phys.* **1943**, *11*, 45; **1944**, *12*, 125.

[83] Ishida M. and Tanaka, F., *Macromolecules* **1997**, *30*, 3900.

[84] Knobler, C.M. and Scott, R. L., in *"Phase Transitions and Critical Phenomena"*, *Vol.9*, Academic Press, New York **1984**.

[85] Pynn, R. and Skjeltorp, A., *"Multicritical Phenomena"*, Plenum Press **1984**.

[86] Wellinghoff, S., Shaw, J. and Baer, E., *Macromolecules* **1979**, *12*, 932.

[87] Tan, H.M., Moet, A., Hiltnet, A. and Baer, E., *Macromolecules* **1983**, *16*, 28.

[88] Boyer, R.F., Baer, E. and Hiltner, A., *Macromolecules* **1985**, *18*, 427.

[89] Domszy, R.C., Alamo, R., Edwards, C.O. and Mandelkern, L., *Macromolecules* **1986**, *19*, 310.

[90] Gan, J.Y.S., Francois, J. and Guenet, J.M., *Macromolecules* **1986**, *19*, 173.

[91] Chen, S.-J., Berry, G.C. and Plazek, D.J., *Macromolecules* **1995**, *28*, 6539.

[92] Winnik, M.A., *Curr. Opin. Colloid Interface Sci.* **1997**, *2*, 424.

[93] Annable, T., Buscall, R., Ettelaie, R. and Whittlestone, D., *J. Rheol.* **1993**, *37*, 695.

[94] Annable, T., Buscall, R., Ettelaie, R., Shepherd, P. and Whittlestone, D., *Langmuir* **1994**, *10*, 1060.

[95] Rao, B., Uemura, Y., Dyke, L. and Macdonald, P.M., *Macromolecules* **1995**, *28*, 531.

[96] Alami, E., Almgren, M., Brown, W. and Francois, J., *Macromolecules* **1996**, *29*, 2229.

[97] Alami, E., Almgren, M. and Brown, W., *Macromolecules* **1996**, *29*, 5026.

[98] Xu, B., Yekta, A. and Winnik, M.A., *Langmuir* **1997**, *13*, 6903.

[99] Tam, K.C., Jenkins, R.D., Winnik, M.A. and Bassett, D.R., *Macromolecules* **1998**, *31*, 4149.

[100] Zhou, Z., Yang, Y.-W., Booth, C. and Chu, B., *Macromolecules* **1996**, *29*, 8357.

[101] Amis, E.J., Hu, N., Seery, T.A.P., Hogen-Esch, T.E., Yassini, M. and Hwang, F., in *"Hydrophobic Polymers: Performance with Environmental Acceptance"*, p.279, ed by E. Glass, Am. Chem. Soc. **1996**.

[102] Hwang, F.S. and Hogen-Esch, T.E., *Macromolecules* **1995**, *28*, 3328.

[103] Xie, X. and Hogen-Esch, T.E., *Macromolecules* **1996**, *29*, 1734.

[104] Zhang, H., Pan, J. and Hogen-Esch, T.E., *Macromolecules* **1998**, *31*, 2815.

[105] Nilsson, S., *Macromolecules* **1995**, *28*, 7837.

[106] Nyström, B., Thuresson, K. and Lindman, B., *Langmuir* **1995**, *11*, 1994.

[107] Nyström, B., Walderhaug, H., Hansen, F.K. and Lindman, B., *Langmuir* **1995**, *11*, 750.

[108] Sarkar, N., *J. Appl. Polym. Sci.* **1979**, *24*, 1073.

[109] Kobayashi, K., Huang, C. and Lodge, T.P., *Macromolecules* **1999**, *32*, 7070.

[110] Morishima, Y., *Trends in Polym. Sci.* **1994**, *2*, 31.

[111] Morishima, Y., Nomura, S., Ikeda, T., Seki, M. and Kamachi, M., *Macromolecules* **1995**, *28*, 2874.

[112] Petit, F., Iliopoulos, I., Audebert, R. and Szonyi, S., *Langmuir* **1997**, *13*, 4229.

[113] Bokias, G., Hourdet, D., Iliopoulos, I., Staikos, G. and Audebert, R., *Macromolecules* **1997**, *30*, 8293.

[114] Bokias, G., Hourdet, D. and Iliopoulos, I., *Macromolecules* **2000**, *33*, 2929.

[115] Fukui, K. and Yamabe, T., *Bull. Chem. Soc. Jpn* **1967**, *40*, 2052.

[116] Tanaka, F. and Stockmayer, W.H., *Macromolecules* **1994**, *27*, 3943.

[117] Tanaka, F. and Koga, T., *Comp. Theor. Polym. Sci.* **2000**, *10*, 259.

[118] Tanaka, F., *J. Polym. Sci., Part B: Polym. Phys.* **2003**, *41*, 2405.

[119] Tanaka, F., *J. Polym. Sci., Part B: Polym. Phys.* **2003**, *41*, 2413.

[120] Gordon, M., *Proc. Roy. Soc. (Lomdon)* **1962**, *A268*, 240 .

[121] Tanaka, F. and Ishida, M., *Macromolecules* **1996**, *29*, 7571.

[122] Eldridge, J.E. and Ferry, J.D., *J. Phys. Chem.* **1954**, *58*, 992.

[123] Tanaka, F. and Nishinari, K., *Macromolecules* **1996**, *29*, 3625.

[124] Nishinari, K. and Tanaka, F., *J. Chim. Phys.* **1996**, *93*, 880.

[125] Flory, P.J., *Proc. R. Soc. London, Ser.A* **1976**, *351*, 351.

[126] Scanlan, J., *J. Polym. Sci.* **1960**, *43*, 501.

[127] Case, L.C., *J. Polym. Sci.* **1960**, *45*, 397.

[128] Pearson, D.S. and Graessley, W.W., *Macromolecules* **1978**, *11*, 528.

[129] Stauffer, D., "*Introduction to Percolation Theory*", Chap.2, Taylor & Francis, London **1985**.

[130] Stossel, T.P., *Sci. Am.* **1994**, *265*, 40.

[131] Clark, A.H., Richardson, R.K., Ross-Murphy, S. and Stubbs, J.M., *Macromolecules* **1983**, *16*, 1367.

[132] Nishinari, K. and Doi, E., *"Food Hydrocolloids: Structures, Properties, and Functions"*, Plenum Press, **1994**.

[133] Indei, T. and Tanaka, F., *J. Rheology* **2004**, to appear in May.

[134] Stockmayer, W.H., *J. Polym. Sci.* **1952**, *9*, 69.

[135] Sperling, L.H., *"Interpenetrating Polymer Networks and Related Materials"*, Plenum Press, **1981**.

[136] Sperling, L.H., *"Multiphase Polymers: Blends and Ionomers"*, ACS Symposium Series *395*, Plenum Press **1988**.

[137] Durrani, C.M., Prystupa, D.A., Donald, A.M. and Clark, A.H., *Macromolecules* **1993**, *26*, 981.

[138] Durrani, C.M. and Donald, A.M., *Macromolecules* **1994**, *27*, 110.

[139] Bokias, G., Hourdet, D., Iliopoulos, I., Staikos, G. and Audebert, R., *Macromolecules* **1997**, *30*, 8293.

PRINTED PAPERS

– Contents –

Review Article

Reprinted Papers

7. A. Matsuyama and F. Tanaka,

Theory of Solvation-Induced Reentrant Coil-Globule Transition of an Isolated Polymer Chain,

J. Chem. Phys. **94**(1), (1991) 781-786.

8. F. Tanaka,

Possible Phase Diagrams for Reversibly Interpenetrating Polymer Networks,

Phys. Rev. Lett. **68**(21), (1992) 3188-3191.

9. F. Tanaka,

Reversible Heteropolymer Gelation – Phase Diagram of Mixed Networks –

in "Ordering in Macromolecular System", ed. by A. Teramoto, M. Kobayashi and T. Norisue,

Springer–Verlag Berlin Heiderberg, (1994) 263-271.

10. F. Tanaka,

Phase Formation of Two-Component Physical Gels,

Physica A **204**, (1994) 660-672.

11. F. Tanaka and W. H. Stockmayer,

Thermoreversible Gelation with Junctions of Variable Multiplicity,

Macromolecules **27**(14), (1994) 3943-3954.

12. F. Tanaka and M. Ishida,

Thermoreversible Gelation of Hydrated Polymers,

J. Chem. Soc. Faraday Trans. **91**, (1995) 2663-2670.

13. F. Tanaka and K. Nishinari,

Junction Multiplicity in Thermoreversible Gelation,

Macromolecules **29**(10), (1996) 3625-3628.

14. K. Nishinari and F. Tanaka,

Structure of Junction Zones in Poly(vinyl alcohol) Gels by Rheological and Thermal Studies,

J. Chim. Phys. **93**, (1996) 880-886.

15. F. Tanaka and M. Ishida,
Elastically Effective Chains in Transient Gels with Multiple Junctions,
Macromolecules **29**(23), (1996) 7571-7580.

16. F. Tanaka,
Phase Formation of Associating Polymers: Gelation, Phase Separation and Microphase Formation,
Adv. Colloid Interface Sci. **63**, (1996) 23-40.

17. F. Tanaka and M. Ishida,
Microphase Formation in Mixtures of Associating Polymers ,
Macromolecules **30**, (1997) 1836-1844.

18. M. Ishida and F. Tanaka,
Theoretical Study of the Post-Gel Regime in Thermoreversible Gelation,
Macromolecules **30**, (1997) 3900-3909.

19. F. Tanaka,
Phase Formation and Dynamics of Associating Polymers,
Prog. Colloid Polym. Sci. **106**, (1997) 158-166.

20. F. Tanaka,
Polymer-Surfactant Interaction in Thermoreversible Gels,
Macromolecules **31**(2), (1998) 384-393.

21. F. Tanaka,
Thermoreversible Gelation of Associating Polymers,
Physica A **257**, (1998) 245-255.

22. F. Tanaka and M. Ishida,
Thermoreversible Gelation with Two-Component Networks,
Macromolecules **32**, (1999) 1271-1283.

23. F. Tanaka,

Polymer-Surfactant Interaction in Thermoreversible Gels,

In "Molecular Interactions and Time-Space Organization in Macromolecular Systems",

Ed. by Y. Marishima, T. Norisuye and K. Tashiro,

Springer–Verlag Berlin Heidelberg, (1998) 81-89.

24. F. Tanaka and T. Koga,

Intramolecular and Intrermolecular Association in Thermoreversible Gelation of Hydrophobically Modified Associating Polymers,

Comp. Theor. Polym. Sci. **10**, (2000) 259-267.

25. F. Tanaka,

Thermoreversible Gelation Strongly Coupled to Polymer Conformational Transition,

Macromolecules **33**(11), (2000) 4249-4263.

26. F. Tanaka and T. Koga,

Theoretical and Computational Study of Thermoreversible Gelation,

Bull. Chem. Soc. Japan **74**(2), (2001) 201-215.

27. T. Nakao, F. Tanaka and S. Kohjiya,

Cascade Theory of Substitution Effects in Nonequilibrium Polycondensation,

Macromolecules **35**(14), (2002) 5649-5656.

28. F. Tanaka,

Intramolecular Micelles and Intermolecular Crosslinks in Thremoreversible Gels of Associating Polymers,

J. Non-Crystalline Solids **307-310**, (2002) 688-697.

29. M. Shoji and F. Tanaka,

Theoretical Study of Hydrogen-Bonded Supramolecular Liquid Crystals,

Macromolecules **35**(19), (2002) 7460-7472.

30. F. Tanaka,

Theoretical Study of Molecular Association and Thermoreversible Gelation in Polymers,

Polymer J. **34**, (2002) 479-509.

31. F. Tanaka,

Thermoreversible Gelation driven by Coil-to-Helix Transition of Polymers,

Macromolecules **36**(14), (2003) 5392-5405 .

32. F. Tanaka,

Gel Formation with Multiple Interunit Junctions I – Molecules carrying Different Functional Groups –,

J. Polym. Sci. Part B: Polym. Phys. **41**, (2003) 2405-2412.

33. F. Tanaka,

Gel Formation with Multiple Interunit Junctions II – Mixture of Different Functional Molecules –,

J. Polym. Sci. Part B: Polym. Phys. **41**, (2003) 2413-2421.

34. F. Tanaka,

Theoretical Study of Helix Induction on a Polymer Chain by Hydrogen-Bonding Chiral Molecules,

Macromolecules, **37**(2), (2004) 605-613.

35. F. Furuya and F. Tanaka,

Effects of Added Surfactants on Thermoreversible Gelation of Associating Polymer Solutions,

J. Polym. Sci. Part B: Polym. Phys. **42**, (2004) 733-751

９４～４５０頁は学術雑誌等に掲載された論文です。出版社から著作権の許諾が得られておりませんので、電子化しておりません。